MCB
Journals.ASM.org

MicroRNA 665 Regulates Dentinogenesis through MicroRNA-Mediated Silencing and Epigenetic Mechanisms

Hannah M. Heair,[a] Austin G. Kemper,[a] Bhaskar Roy,[a] Helena B. Lopes,[b] Harunur Rashid,[a] John C. Clarke,[a] Lubana K. Afreen,[a] Emanuela P. Ferraz,[b] Eddy Kim,[a] Amjad Javed,[a] Marcio M. Beloti,[b] Mary MacDougall,[a] Mohammad Q. Hassan[a]

Department of Oral and Maxillofacial Surgery, Institute of Oral Health Research, School of Dentistry, University of Alabama at Birmingham, Birmingham, Alabama, USA[a]; Cell Culture Laboratory, School of Dentistry of Ribeirão Preto, University of São Paulo, Ribeirão Preto, São Paulo, Brazil[b]

Studies of proteins involved in microRNA (miRNA) processing, maturation, and silencing have indicated the importance of miRNAs in skeletogenesis, but the specific miRNAs involved in this process are incompletely defined. Here, we identified miRNA 665 (miR-665) as a potential repressor of odontoblast maturation. Studies with cultured cell lines and primary embryonic cells showed that miR-665 represses the expression of early and late odontoblast marker genes and stage-specific proteases involved in dentin maturation. Notably, miR-665 directly targeted *Dlx3* mRNA and decreased *Dlx3* expression. Furthermore, RNA-induced silencing complex (RISC) immunoprecipitation and biotin-labeled miR-665 pulldown studies identified *Kat6a* as another potential target of miR-665. KAT6A interacted physically and functionally with RUNX2, activating tissue-specific promoter activity and prompting odontoblast differentiation. Overexpression of miR-665 reduced the recruitment of KAT6A to *Dspp* and *Dmp1* promoters and prevented KAT6A-induced chromatin remodeling, repressing gene transcription. Taken together, our results provide novel molecular evidence that miR-665 functions in an miRNA-epigenetic regulatory network to control dentinogenesis.

Dentinogenesis is the process by which dentin, the major mineralized tissue of teeth, is formed through progressive cytodifferentiation of progenitor cells to mature odontoblasts (1). Multiple layers of gene regulation, including those by microRNA (miRNA), orchestrate the physiologic process of dentinogenesis in a stage-specific manner (2). Progenitor cells, including dental papilla cells or dental follicle cells, derived from the ectomesenchyme of the cranial neural crest, differentiate into preodontoblasts and produce predentin. Predentin stimulates further differentiation of the cells it surrounds, giving rise to mature odontoblasts that produce dentin. Odontoblast secretion of dentin extracellular matrix proteins, including dentin sialophosphoprotein (DSPP) and dentin matrix protein 1 (DMP1), aids in the process of mineralization that forms primary dentin. However, the mechanisms of odontoblast-specific gene regulation by miRNA during dentinogenesis are not clearly understood.

miRNAs are endogenous, noncoding RNAs implicated in posttranscriptional RNA silencing (3–9). The importance of miRNAs in skeletogenesis has been shown in mice by loss-of-function analysis of proteins involved in miRNA processing (Drosha and DGCR8), maturation (Dicer), and silencing (argonaute 2; AGO2), which revealed embryonic lethality and severe developmental defects upon loss of these proteins (10–15). Furthermore, cartilage-specific deletion of Dicer led to accelerated differentiation and subsequent cell death (11), whereas osteoblast- and osteoclast-specific deletion increased bone mass (13, 16). Current studies on miRNA regulation of gene expression indicate a key role for this process in tooth development (17–20) and in controlling cellular signaling (18, 21–25) and differentiation (2, 26). However, these studies have not defined the contributions of miRNA-mediated epigenetic control during odontoblast differentiation. MicroRNA 665 (miR-665) located on human chromosome 14 clusters closely with miR-337, which has been implicated in chondrogenesis; however, there has been no report on the role of miR-665 in tooth formation (27).

Studies from several research groups have revealed that homeodomain gene *Dlx3* (Online Mendelian Inheritance in Man [OMIM] entry 600525) is a highly critical regulator of craniofacial and postnatal skeletal development (28–34). Mutations in *DLX3* in humans have been associated with tricho-dento-osseous syndrome (TDO; OMIM 190320) and amelogenesis imperfecta with taurodontism (AIHHT; OMIM 104510), both of which are conditions characterized by abnormalities in tooth formation (35–39). During development, *Dlx3* expression occurs in cranial neural crest cells, endochondral osteoblasts, odontoblasts, ameloblasts, hypertrophic chondrocytes, and the developing limb (40, 41), and *Dlx3*-knockout mice die from placental failure at embryonic day 9.5 (E9.5), prior to bone and tooth formation (28). Expression of DLX3 in postmigratory neural crest cells (E9.5) helps commit these cells to further differentiate into odontoblasts and cementoblasts, contributing to formation of mature dentin and cementum for proper tooth formation (40). Recently, *Dspp* was identified as a direct target of

Received 26 January 2015 **Returned for modification** 11 February 2015
Accepted 18 June 2015

Accepted manuscript posted online 29 June 2015

Citation Heair HM, Kemper AG, Roy B, Lopes HB, Rashid H, Clarke JC, Afreen LK, Ferraz EP, Kim E, Javed A, Beloti MM, MacDougall M, Hassan MQ. 2015. MicroRNA 665 regulates dentinogenesis through microRNA-mediated silencing and epigenetic mechanisms. Mol Cell Biol 35:3116–3130. doi:10.1128/MCB.00093-15.

Address correspondence to Mohammad Hassan, hassank@uab.edu.

H.M.H. and A.G.K. contributed equally to this article.

Supplemental material for this article may be found at http://dx.doi.org/10.1128/MCB.00093-15.

doi:10.1128/MCB.00093-15

DLX3 in odontoblasts (30). This is the first mechanistic link established between the transcription factor DLX3 and the dentin matrix protein DSPP, both known to be mutated in human disorders associated with tooth abnormalities (29, 30). Despite the known role of DLX3 in the development of bone and tooth phenotypes, the mechanism(s) of the posttranscriptional regulation of *Dlx3* by miRNA during dentinogenesis is still unclear.

K (lysine) acetyltransferase 6a (KAT6A), also referred to as MOZ or MYST-3, is a founding member of the MYST family of lysine acetyltransferases, defined by a conserved MYST/MOZ domain (42). Functionally, KAT6A acetylates both itself and lysine residues on histones H2B, H3, and H4 (43–46). Furthermore, KAT6A functions as a coactivator for several DNA-binding transcription factors including RUNX1 (44, 47–50) and RUNX2 (51), which perform a crucial role in osteogenesis (52, 53). *Moz/Kat6a* deletion is embryonic lethal (49), and haploinsufficiency for *Moz/Kat6a* demonstrated craniofacial abnormalities (54, 55). Additionally, *Moz/Kat6a*-knockout mouse model studies suggest that a Moz-driven acetylation mechanism controls a balance between cellular proliferation and differentiation (56).

In this study, we found miR-665 to be a potential repressor of odontoblast maturation through inhibition of *Dlx3* and *Kat6a* translation and increased mRNA degradation. The expression of miR-665 is temporal and reciprocal to DLX3 and RUNX2 expression during *in vitro* odontoblast differentiation. Direct binding of RUNX2 in the miR-665 promoter negatively regulates expression of miR-665, and miR-665 promotes the switch from acetylation to methylation of H3K9 in the tooth-specific *Dspp* and *Dmp1* promoters, further reducing the recruitment of active transcription factors and chromatin modifiers. Conversely, KAT6A acetylates and physically interacts with RUNX2 to functionally modulate RUNX2 transcriptional activity and promote dentinogenesis. By reducing both DLX3 and KAT6A expression, miR-665 hinders the formation of activating complexes to promote epigenetic activation of *Dspp* and *Dmp1* chromatin, impairing odontoblast differentiation.

MATERIALS AND METHODS

Cell culture. HEK-293T, rat dental pulp MDPC-23, and rat odontoblast OD-21 cells (57) were cultured at 37°C, and mouse odontoblast-like M06-G3 cells (58) were maintained at 33°C, all in 5% CO_2 in Dulbecco's modified Eagle's medium (DMEM) supplemented with 4.5 g/liter glucose, L-glutamine, sodium pyruvate (Cellgro, VA), 10% fetal bovine serum (Atlanta Biologicals, GA), 100 μg/ml streptomycin, 100 units/ml penicillin (Gibco, NY), and 250 μg/ml amphotericin B (Cellgro, VA). To induce differentiation, medium was further supplemented with 50 μg/ml ascorbic acid, 10 mM β-glycerophosphate, and 1×10^{-7} M dexamethasone (Sigma-Aldrich, St. Louis, MO) for up to 21 days. Medium was refreshed every 48 h for the duration of all experiments. Cell layers were fixed in 2% paraformaldehyde or 10% formalin for histochemical detection of alkaline phosphatase (ALP) using Sigma reagents.

The levels of miR-665 expression were very similar in all three odontoblast cell lines we tested (see Table S1 in the supplemental material). The evidence for miR-665 function in several cell lines justifies the significance of our studies and provides information for future mouse model development.

***Dlx3* and *Kat6a* 3′ UTR-reporter constructs and transfection.** The *Dlx3* 3′ untranslated region (UTR; 1.5 kb) fragment was amplified with overhanging 5′ EcoRI and 3′ NotI restriction sites. DNA fragments were phosphorylated and ligated into the EcoRI-NotI sites of the pMIR-REPORT luciferase (Luc) plasmid (Applied Biosystems, Inc., Foster City, CA) to generate the *Dlx3* 3′ UTR-Luc reporter plasmid. M06-G3 cells at 30% to 50% confluence were transfected with double-stranded RNA oligonucleotides representing mature sequences that mimic endogenous miR-9, miR-320, miR-421, or miR-665 or an miRNA nonspecific (NS) control (obtained from Switchgear Genomics, Menlo Park, CA). MDPC-23 or OD-21 cells at 30% to 50% confluence were transfected with miR-665, anti-miRNA, or NS miRNAs. Luc assays were performed with M06-G3 cells cotransfected with the specified miRNAs (100 nM each) or NS miRNA (100 nM) and the *Dlx3* 3′ UTR-Luc reporter DNA (200 ng) plasmid using 5 μl of RNAiMax (Invitrogen, Carlsbad, CA) in three independent experiments. *Dspp*, *Sp7*, and *Runx2* promoter-Luc assays were performed in a similar manner by using 100 ng of promoter-Luc DNA cotransfected with 50 ng of control or *Kat6a* (Fisher Scientific, Pittsburgh, PA), *Dlx3*, or *Runx2* (31) overexpression construct. Data represent the means and standard errors of the means (SEM) for three experiments and samples. The transfected cells were incubated for 24 h to determine Luc activity or harvested after 48 h for protein and mRNA analysis. Transfection with *Renilla* Luc plasmid (Promega, Madison, WI) was used to normalize the relative Luc values. Relative Luc activity (firefly Luc activity/*Renilla* Luc activity) was expressed in relative luminescence units and plotted. To characterize the specificity of miR-665 binding, the 3′ UTRs (90 to 100 bp) of putative targets *Dlx3* and *Kat6a* were synthesized with flanking 5′ SpeI and 3′ HindIII restriction sites. Double-stranded annealed DNA fragments were phosphorylated and ligated to the pMIR-REPORT Luc plasmid. Transformants were grown, and plasmid DNAs were confirmed by sequencing. Luc assays were conducted by cotransfecting miR-665 (100 ng), NS miRNA (100 ng), or anti-miR-665 (100 ng) with a wild-type (WT) or mutant *Dlx3* or *Kat6a* 3′ UTR-Luc reporter DNA (200 ng) construct into HEK-293T cells. WT and mutant sequences of each 3′ UTR are shown in Table S2 in the supplemental material. A *Renilla* Luc plasmid (Promega) was transfected to normalize the relative Luc values. The transfected cells were incubated for 24 h to determine Luc activity.

Generation of cells stably expressing miR-665 and anti-miR-665. Lentiviral miR and anti-miRNA precursor clones (CD-511B-1 for control, MMIR-665-PA-1 for miR-665 overexpression, and MiRZIP665-PA-1 for miR-665 knockdown; System Biosciences, Mountain View, CA) were used to produce mature virus particles expressing green fluorescent protein (GFP) and miR-665 or anti-miR-665. The pCDH-*Dlx3* lentiviral clone (System Biosciences) was used to generate virus particles expressing *Dlx3* and coexpressing GFP. For viral packaging, individual lentiviral clones were cotransfected with pMD2.G and pCMVΔR-8.91 viral packaging plasmids (Addgene plasmids 12259 and 12263; Addgene, Cambridge, MA) into HEK-293T cells. Viral supernatants were harvested 48 h after transfection and subsequently used for infections. Mouse and rat odontoblasts were infected at 60% to 70% confluence for 48 h. Expression of the GFP reporter was monitored and used to sort cells expressing miR-665, anti-miR-665, or DLX3. Cells were then seeded into six-well plates and differentiated for 7 days.

RNA isolation and real-time RT-qPCR. Total RNA was isolated using TRIzol reagent (Invitrogen, Grand Island, NY) according to the manufacturer's specifications. DNase I-treated total cellular RNA was primed with oligo(dT) or random hexamer and reverse transcribed into cDNA using a SuperScript III first-strand synthesis kit (Invitrogen, Grand Island, NY) according to the manufacturer's instructions. For miRNA detection, poly(A) tailing was performed using a poly(A) polymerase (Pol) kit (Ambion, Grand Island, NY) according to the manufacturer's instructions, and reverse transcription was carried out with a SuperScript III first-strand synthesis kit according to the manufacturer's instructions. Gene expression was determined by real-time reverse transcriptase quantitative PCR (RT-qPCR) using Power SYBR green PCR master mix (Applied Biosystems, Inc.) and gene-specific primers in an ABI Prism 7000 Fast thermocycler. For each gene, expression levels were normalized to glyceraldehyde-3-phosphate dehydrogenase (GAPDH) or U6 RNA expression. Experiments were performed in triplicate, and results are given as mean

values ± SEM. Nucleotide sequences of primers are provided in Table S3 of the supplemental material.

Antibodies. The antibodies used for Western blotting, chromatin immunoprecipitation (ChIP) assays, and ribonucleoprotein immunoprecipitation (RNP-IP) are listed in Table S4 of the supplemental material.

Western blot analysis. Cells were lysed in radioimmunoprecipitation assay (RIPA) lysis buffer (25 mM Tris-HCl [pH 7.6], 150 mM NaCl, 1% NP-40, 1% sodium deoxycholate, 0.1% SDS, 1 mM phenylmethylsulfonyl fluoride, 1× protease inhibitor cocktail [Roche], and 25 μM MG132 [proteasome inhibitor]). Lysates were sonicated three times on ice at 2% power for 10 s. Samples (cleared lysates) were quantified, and equal amounts of protein were resolved by SDS-PAGE. Proteins were transferred to a polyvinylidene difluoride (PVDF) membrane and were subjected to immunoblotting with the appropriate antibodies. Immunoreactive proteins were detected using Western Lightning chemiluminescence reagent (Perkin-Elmer, Boston, MA).

RNP-IP. Polysomal extracts from OD-21 or MDPC-23 cells overexpressing miR-665 or anti-miR-665 were immunoprecipitated with affinity-purified silencing complex-specific anti-AGO2 antibody (Millipore) as previously described (59–69). The RNA isolated from RNP-IP was subjected to cDNA synthesis using primers derived from a specific seed sequence for miR-665. The first-strand cDNA was further amplified with forward and reverse primers derived from the immediate upstream sequence of the 3′ UTR target region of the *Dlx3* mRNA.

Next-generation mRNA sequencing. The total RNA was purified from the AGO2-immunoprecipitated complex isolated from control, miR-665-overexpressing, and anti-miR-665-overexpressing MDPC-23 or OD-21 cells and subjected to mRNA sequencing in an Illumina HiSeq 2000 system (Illumina, San Diego, CA) using the latest versions of the sequencing reagents and flow cells to provide up to 300 Gb of sequence information per flow cell. The quality of the immunoprecipitated RNA was assessed using an Agilent 2100 Bioanalyzer (Agilent, Santa Clara, CA) before conversion to cDNA. TruSeq library generation kits were used according to the manufacturer's instructions (Illumina). Library construction consisted of random fragmentation of the miRNA followed by cDNA production using random primers. The ends of the cDNA were repaired and poly(A) tailed, and adaptors were ligated for indexing (up to 12 different bar codes per lane) during the sequencing runs. The cDNA libraries were quantitated using qPCR in a Roche LightCycler 480 with a Kapa Biosystems (Woburn, MA) kit before cluster generation. Clusters were generated to yield approximately 725,000 to 825,000 clusters/mm^2. Cluster density and quality were determined during the run after the parameters of the first base addition were assessed. Paired-end 2- by 50-bp sequencing runs were conducted to align the cDNA sequences to the reference genome. Before alignment, the data were converted to the FASTQ Sanger format using FASTQ Groomer. TopHat was used to align high-throughput sequencing reads of RNA transcripts (RNA-Seq) to the reference genome using the short-read aligner Bowtie and to analyze the mapping results to identify splice junctions between exons. Aligned reads from TopHat were analyzed by Cufflinks to assemble transcripts, estimate transcript abundances, and test for differential expression and regulation. Cuffcompare, which is part of Cufflinks, was then used to compare the assembled transcripts to a reference annotation and track Cufflinks transcripts across multiple experiments. Finally, Cuffdiff was used to indicate significant changes in transcript expressions, splicing, and promoter use. To call small nucleotide polymorphisms, SAM Tools was used. Briefly, the BAM file generated by TopHat was filtered so that the read was paired and mapped. A pileup file was created from this filtered file, and the consensus was generated using the MAQ model. This pileup file was then filtered to report variants as well as to convert coordinates to intervals that were covered by a specified number of reads with bases above a set quality threshold.

ChIP assays. ChIP assays were performed as previously described (31, 70). Briefly, formaldehyde cross-linking of DNA-bound proteins in miR-665-overexpressing and anti-miR-665-overexpressing odontoblasts was performed for 15 min. Cells were collected in 1× phosphate-buffered saline (PBS) and then lysed in lysis buffer (25 mM Tris-HCl [pH 8.0], 5 mM $MgCl_2$, 10 mM EDTA, 1% SDS, 1% Triton X-100, 162.5 mM NaCl, 25 μM MG-132, and 1× complete protease inhibitor). Cell lysates were sonicated to obtain DNA fragments with an average size of 0.2 to 0.6 kbp. Immunoprecipitations were performed with the appropriate antibodies or immunoglobulin G (IgG) as a control (see Table S4 in the supplemental material). Immune complexes were collected, followed by recovery of DNA. Aliquots of each recovered DNA sample were assayed by qPCR to detect the proximal *Dspp* and *Dmp1* promoter regions upstream of the transcription start site. The oligonucleotide primers used are listed in Table S3 of the supplemental material. Samples were normalized to the initial input and expressed as percent chromatin pulldown (compared with input). ChIP experiments were repeated three times with similar results, and data in the Fig. 7 are the averages of three experiments with SEM.

Immunoprecipitation. Approximately 10^7 cells per immunoprecipitation were lysed in 500 μl of Nonidet P-40 (NP-40) lysis buffer (150 mM NaCl, 50 mM Tris [pH 8.0], 1% NP-40, 1× complete protease inhibitor, and 25 μM MG-132) for 15 min at 4°C. Cell lysates were sonicated, followed by centrifugation at 16,000 × *g* for 15 min at 4°C. The supernatant was transferred to a clean microcentrifuge tube and precleared with 40 μl of protein A/G plus agarose beads (Santa Cruz) at 4°C for 30 min. To precipitate immunocomplexes, 5 to 10 μg of antibody was added and incubated at 4°C with agitation for 4 h or overnight. Sixty microliters of protein A/G plus agarose beads (100 μl of 1:1 beads-PBS) was added to the antibody-protein solution, and the cross-linking reaction was performed at room temperature for 1 h. Beads were washed three times with 1× PBS containing 1× protease inhibitors and 50 μl of 2× sample buffer, followed by boiling for 5 min before analysis by Western blotting.

Biotin pulldown. A biotin pulldown assay was performed to isolate *Dlx3* and *Kat6a* mRNAs that bind to transfected biotinylated miR-665 (Bi-miR-665) (68, 69). MDPC-23 cells (0.2 × 10^6 cells/well) were transfected in triplicate with 100 pmol/well biotinylated nonspecific miRNA (Bi-NS-miR) or biotinylated miR-665 (Bi-miR-665) (Integrated DNA Technologies, Inc.) in six-well plates. Thirty-six hours later, the cells from three wells were harvested and centrifuged at 2,000 × *g*. After three washes with 1× PBS, cell pellets were lysed in 0.7 ml of lysis buffer (20 mM Tris [pH 7.5], 100 mM KCl, 5 mM $MgCl_2$, 0.3% NP-40, 80 U of RNase Out [Invitrogen], and Halt protease inhibitor cocktail [Life Technologies]), and incubated on ice for 10 min. Lysates were sonicated on ice at 2% power for 10 s three times, followed by centrifugation at 10,000 × *g* for 15 min at 4°C. The supernatant was transferred to a clean microcentrifuge tube. Streptavidin-coated magnetic beads (Invitrogen) were blocked in lysis buffer containing 500 μg/ml *Saccharomyces cerevisiae* tRNA and 1 mg/ml bovine serum albumin (BSA; Promega) for 2 h at 4°C and then washed twice with 1 ml of lysis buffer. To capture miR-665-bound target mRNA, cytoplasmic lysate was added to 100 μl of beads and incubated for 4 h at 4°C in a tube rotator. Beads were washed three times with lysis buffer containing 1× protease inhibitors. RNA bound to the beads (pulldown RNA) or from 10% of the cleared lysate (input RNA) was isolated using TRIzol (Invitrogen). The levels of Dlx3 and Kat6a mRNAs in the Bi-miR-665 or Bi-NS-miR pulldown assays were quantified by RT-qPCR. GAPDH was used to normalize the mRNA levels. The fold enrichment of pulldown mRNA from Bi-miR-665-transfected cells over that from Bi-NS-miR-transfected cells was plotted.

RESULTS

Discovery of miR-665. A single miRNA is expected to target a large number of diverse mRNAs; each singular mRNA may be regulated by at least 15 distinct miRNAs (71–73). To overcome this target multiplicity and aid in the selection of *Dlx3*-targeting miRNAs that contribute to dentinogenesis, several principles were implemented: (i) multiple miRNA bioinformatics algorithms (PicTar, TargetScan, and microRNA.org) were utilized to identify

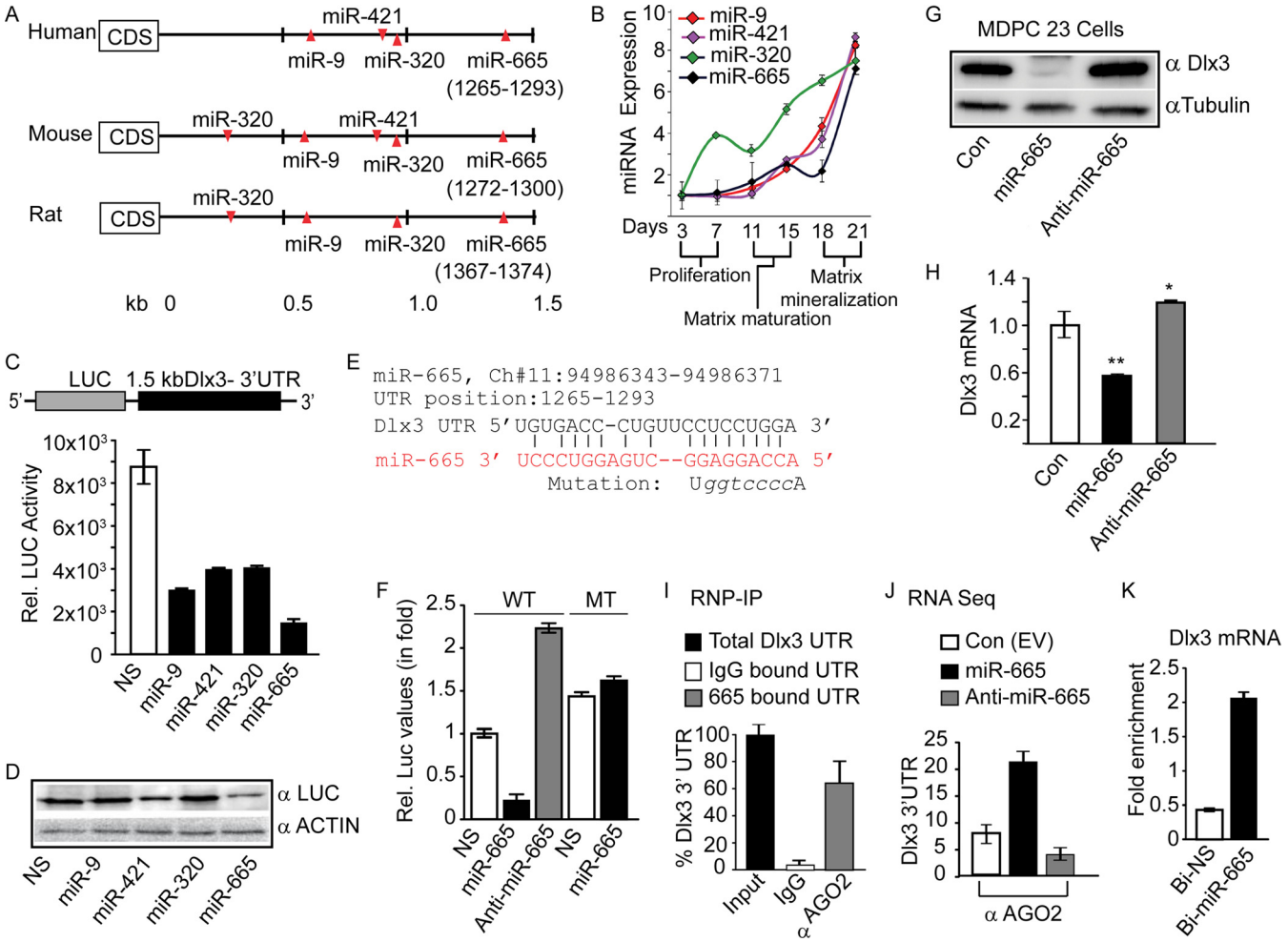

FIG 1 Identification of a functional miR-665 site in the *Dlx3* mRNA 3′ UTR. (A) Putative binding sites for miR-9, miR-320, miR-421, and miR-665 (within 1.5 kb distal to the stop codon) conserved across mammalian species identified in *Dlx3* mRNA using bioinformatics programs (http://useast.ensembl.org/Mus_musculus/Gene/Summary). Nucleotide positions for miR-665 are shown in parentheses. (B) Relative expression levels of miR-9, miR-320, miR-421, and miR-665 obtained by real-time RT-qPCR using total RNA isolated from mouse odontoblasts (M06-G3) induced to differentiate for 21 days. U6 RNA was used as a loading control. (C) Schematic representation of the *Dlx3* 3′ UTR-Luc reporter vector created by cloning the *Dlx3* 3′ UTR (1.5 kb) into the pMIR-REPORT Luc reporter vector (top). Relative Luc activity was determined in lysates from M06-G3 cells transfected with *Dlx3* 3′ UTR-Luc, nonspecific (NS) miRNAs, and individual *Dlx3*-targeting miRNAs (bottom). Luc activity was normalized with *Renilla* Luc activity and expressed in relative luminescence units. (D) Representative Western blot analysis with anti-Luc antibody of lysates from M06-G3 cells transfected with *Dlx3* 3′ UTR-Luc and individual *Dlx3*-targeting miRNAs. (E) Alignment of miR-665 binding to the murine *Dlx3* 3′ UTR. Lowercase nucleotides indicate the mutations introduced in the seed sequence of the miR-665 binding site within *Dlx3*. (F) Relative Luc activity in HEK-293T cells transfected with wild-type (WT) or mutated (MT) *Dlx3* 3′ UTR constructs along with nonspecific miRNA control (NS), miR-665, or anti-miR-665. Relative Luc activity was normalized with *Renilla* Luc activity and expressed in relative luminescence units. (G) Representative Western blot showing DLX3 protein expression in MDPC-23 dental pulp cells stably infected with control, miR-665-expressing, or anti-miR-665-expressing lentiviral particles. Tubulin was used as a loading control. (H) Quantitative analysis of the relative *Dlx3* mRNA expression levels, normalized to *Gapdh*, in MDPC-23 dental pulp cells stably infected with control, miR-665-expressing, or anti-miR-665-expressing lentiviral vectors, detected by qPCR after 96 h. *, $P \leq 0.05$; **, $P \leq 0.01$. (I) Representative RNP-IP assay in MDPC-23 cell lysates incubated with IgG (control) or anti-AGO2 antibody. Data are presented as the amount of miR-665 bound to the *Dlx3* 3′ UTR fragment (gray bar) relative to the total *Dlx3* 3′ UTR cDNA input (black bar). Normal IgG was used as a negative control. The RISC was immunoprecipitated with anti-AGO2 antibody, and associated mRNA was reverse transcribed to cDNA, using the miR-665 seed sequence as a primer, and amplified by real-time RT-qPCR with primers specific to miR-665 binding sites in the *Dlx3* 3′ UTR. (J) Quantitative analysis of miR-665 binding to the *Dlx3* 3′ UTR associated with the RISC determined by RNA sequencing of AGO2-immunoprecipitated RNA from MDPC-23 dental pulp cells transduced with control, miR-665-overexpressing, and anti-miR-665-expressing lentiviral vectors. Significant changes in transcript expression (*P* values of 0.01 to 0.001) were analyzed using Cuffdiff bioinformatics. (K) Streptavidin pulldown to detect *Dlx3* mRNA binding to miR-665 in MDPC-23 odontoblast cells transfected with Bi-NS-miR or Bi-miR-665 mimics. The binding of *Dlx3* mRNA was analyzed by qRT-PCR and normalized to *Gapdh* expression. CDS, coding DNA sequence; Ch, chromosome; LUC, luciferase; CON, control; UTR, untranslated region; EV, empty vector; Bi, biotinylated.

potential miRNAs; (ii) the binding sites were chosen between the stop codon and poly(A) site of the *Dlx3* mRNA for optimal silencing potential (73); and (iii) miRNA qPCR analysis was used to validate the expression of the identified miRNAs in odontoblasts. Four miRNAs (miR-9, miR-320, miR-412, and miR-665) met our predefined criteria for *Dlx3*-targeting miRNAs. All four miRNAs bind regions located between kb +0.1 and kb +1.5 of the *Dlx3* 3′ UTR (Fig. 1A), and expression of each miRNA was detected in an odontoblast-like cell line (Fig. 1B). Analysis of the temporal expression patterns of these miRNAs in M06-G3 odontoblast-like

cells revealed very low expression of miR-9, miR-665, and miR-421 from the proliferation stage to the mature odontoblast stage, a period ranging up to day 15 after induction of differentiation. Maximum expression of the same miRNAs was observed during the mineralization stage, ranging from 18 to 21 days after induction of differentiation. An initial increase in the expression of miR-320 was found in proliferating odontoblasts (differentiation days 3 to 7), followed by a slight decline at maturation (day 11) and a second induction in more mature odontoblasts (differentiation days 12 to 21). These findings strongly indicate that miR-665, miR-9, miR-421, and miR-320 could potentially regulate *Dlx3* expression in odontoblast cells during differentiation.

To examine the specificity and efficacy of these miRNAs, we cloned a 1.5-kb fragment of the *Dlx3* 3′ UTR into the 3′ UTR of a Luc reporter gene to create the *Dlx3* 3′ UTR-Luc plasmid. Lysates from M06-G3 cells transfected with miR-9, miR-320, miR-421, or miR-665 and the *Dlx3* 3′ UTR-Luc plasmid were assayed for Luc reporter activity. Exogenous expression of each miRNA substantially repressed Luc activity. However, miR-665 induced the greatest repression (Fig. 1C). Lysates from M06-G3 cells transfected with miR-9, miR-320, miR-421, or miR-665 and the *Dlx3* 3′ UTR-Luc plasmid were also subjected to immunoblot analysis with an anti-Luc antibody. Exogenous expression of miR-665 and miR-421 substantially repressed Luc protein expression. However, no effects on Luc protein expression were observed after overexpression of miR-320 or miR-9 (Fig. 1D). RNA nucleotide complementarity analysis of miR-665 binding to the *Dlx3* 3′ UTR indicated an imperfect RNA, an RNA hybrid, appropriate for miRNA-mediated repression (Fig. 1E). Primarily, miRNAs bind to the 3′ UTR of mRNAs and repress translation; therefore, we mutated the functional miR-665 binding site in *Dlx3* and investigated the effects using the *Dlx3* 3′ UTR-Luc reporter assay in HEK-293T cells. Substantial downregulation of Luc activity (80% to 90%) was detected when the WT *Dlx3* 3′ UTR-Luc plasmid was coexpressed with miR-665 (Fig. 1F), but downregulation did not occur when the miR-665 binding site in the *Dlx3* 3′ UTR was mutated. In contrast to the effects of miR-665 overexpression, anti-miR-665 overexpression increased Luc activity by at least 2-fold. These results indicate that miR-665 directly regulates homeobox factor *Dlx3* through an miRNA-mediated mechanism. Based on the above findings and the higher expression of miR-665 in odontoblast and other mineralized cells and tissue (see Table S1 in the supplemental material), we chose to study the function of miR-665 in odontoblast differentiation.

The ability of miR-665 to target and silence endogenous *Dlx3* was further validated by miR-665 overexpression and knockdown assays. In MDPC-23 dental pulp cells, overexpression of miR-665 substantially repressed endogenous *Dlx3* expression (at the mRNA and protein levels), whereas expression of anti-miR-665 increased *Dlx3* expression (Fig. 1G and H). To study the *in vivo* binding of miR-665 to the 3′ UTR of *Dlx3* mRNA, we performed an RNP-IP pulldown assay. In miR-665-overexpressing MDPC-23 cells, a significant level (60%) of *Dlx3* mRNA was bound by miR-665 (Fig. 1I), as determined by real-time RT-qPCR analysis of immunoprecipitated RNA. Additionally, sequencing of the RNP-IP RNA revealed 8- and 2.5-fold enrichments in miR-665 binding to the *Dlx3* 3′ UTR in miR-665-overexpressing cells compared with anti-miR-665- and control lentivirus-overexpressing cells, respectively (Fig. 1J). To exclude the possibility that the 3′ UTR of *Dlx3* mRNA is recovered because of binding to miRNAs other than miR-665, we transfected MDPC-23 cells with biotinylated miR-665 (Bi-miR-665). Analysis of RNA pulled down by streptavidin beads (streptavidin pulldown RNA) by RT-qPCR revealed a substantial increase (4-fold) in *Dlx3* mRNA pulled down with Bi-miR-665 over the amount pulled down with the biotinylated nonspecific miRNA (Fig. 1K). Thus, these results indicate that *Dlx3* expression is directly controlled posttranscriptionally through 3′ UTR regulation by miR-665. Therefore, we concluded that miR-665 is well positioned to have a central role in the regulation of odontoblast differentiation.

miR-665 expression profile opposes *Dlx3* and odontoblast differentiation. Because miR-665 directly targets *Dlx3*, we hypothesized that there is a functional yin-yang relationship in the expression of miR-665 and *Dlx3* expression during dentinogenesis. We tested the expression of both in differentiating M06-G3 odontoblast-like and primary dental pulp cells and in mouse embryonic endochondral bone (Fig. 2). The appropriate differentiation of M06-G3 and dental pulp cells was confirmed by the expression of the odontoblast stage-specific marker genes *Runx2*, *Dlx3*, and *Dspp* (see Fig. S1 in the supplemental material). In odontoblast-like cells, endogenous miR-665 expression was low in the odontoprogenitor and mature odontoblast stages (up to differentiation day 11) and high during the mineralization stage (differentiation days 15 to 21). Correlating inversely with low miR-665 RNA levels, expression of DLX3 peaked in proliferating to mature odontoblasts (differentiation days 4 to 11). However, miR-665 expression increased as DLX3 expression declined at the mineralization stage (Fig. 2A). Similar profiles of expression for miR-665 and DLX3 were observed in primary dental pulp cells during proliferation to early maturation (differentiation days 0 to 10) and at mineralization (Fig. 2B). The same reciprocal correlation was noticed during skeletogenesis (embryonic days E12 to E19) (Fig. 2C). To address whether the biological control of miR-665 increases during differentiation, as suggested in by the experiment shown in Fig. 2B, we performed RNP-IP in primary human dental pulp cells at day 7 (early) and at day 10 (late) of differentiation. RNP-IP at later days of differentiation (e.g., day 15) is challenging because of a high extracellular matrix content. Binding of miR-665 to the *DLX3* mRNA 3′ UTR was 3-fold lower at day 7 than at day 10 of differentiation (Fig. 2D), reflecting the lower protein level of DLX3 observed at this time (Fig. 2B). These results indicate a requirement for miR-665 biological regulation of *Dlx3* expression during dentinogenesis.

Next, we examined the effects of osteogenic factors, bone morphogenic protein 2 (BMP2; 200 ng/ml), $1,25(OH)_2D_3$ (vitamin D; 10^{-5} unit/ml), dexamethasone (10 ng/ml), or all-*trans* retinoic acid (2 μM) on the expression of miR-665. miR-665 expression was decreased 50% by treatment with BMP2 for 24 h, and lesser but significant changes in miR-665 expression were observed after treatment with vitamin D, dexamethasone, or retinoic acid (Fig. 2E). Thus, BMP2 and other anabolic agents that support skeletogenesis downregulate miR-665 expression. Previously, we reported that RUNX2, the master regulator of bone and tooth formation, negatively regulates miR-23a cluster expression to promote osteoblast differentiation (70). Thus, we explored the possibility that RUNX2 negatively regulates miR-665 expression to promote dentinogenesis. Mouse calvaria osteoblasts from *Runx2*-null mice (52) showed more than 7-fold higher miR-665 expression than osteoblasts from WT mice, and reintroduction of

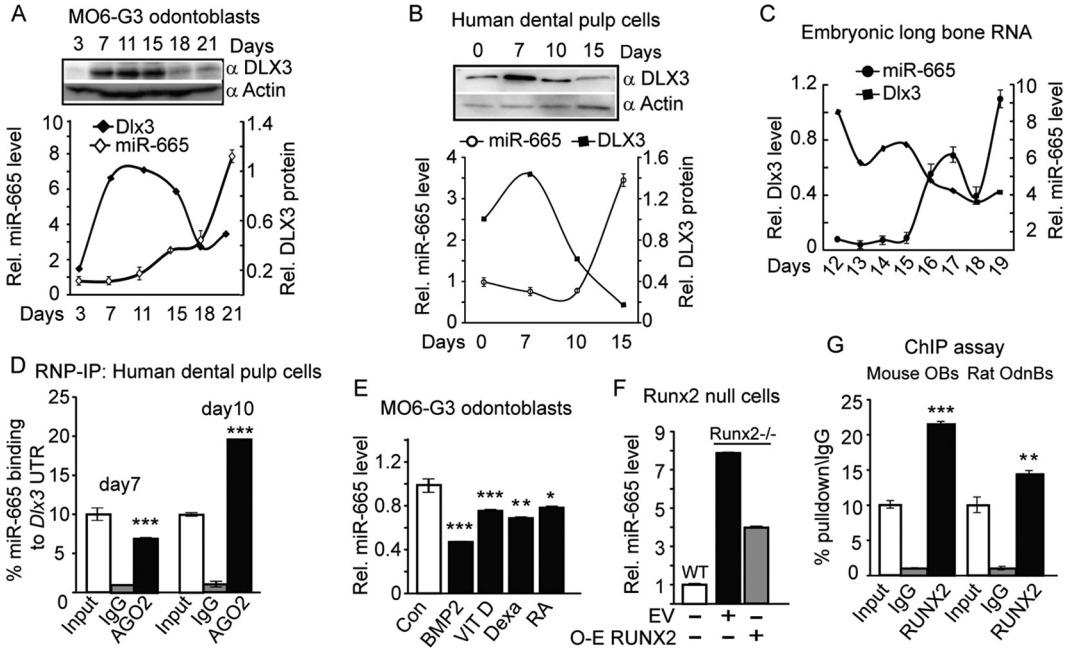

FIG 2 Temporal expression of miR-665 and DLX3 maintains the physiology of odontoblast differentiation. (A) Representative Western blot showing DLX3 protein from M06-G3 cell lysates at the indicated days of differentiation (top). The graph depicts the relative expression levels of *Dlx3* and miR-665 during M06-G3 differentiation, normalized to actin (bottom). (B) Representative Western blot showing total protein from primary human dental pulp cells assayed for DLX3 expression at the indicated days of differentiation (top). The graph depicts the relative expression levels of *DLX3* and miR-665 during primary human dental pulp cell differentiation, normalized to actin (bottom). (C) Total RNA isolated from mouse long bones at the indicated times of embryonic development was analyzed for the expression of miR-665 and *Dlx3* by real-time RT-qPCR. *U6* expression was used as the loading control. (D) *In vivo* miR-665 binding to *DLX3* 3′ UTR detected by RNP-IP with anti-AGO2 antibody. The 3′ UTR of *DLX3* mRNA associated with AGO2 was amplified with primers specific to the miR-665 binding sites (see Table S3 in the supplemental material). Normal IgG and 10% input were used as negative and positive controls, respectively. (E) Effects of osteogenic factors on the expression of miR-665 in MDPC-23 dental pulp cells. Relative miR-665 expression was assessed with real-time RT-qPCR analysis of total cellular RNA from odontoblasts treated with BMP2 (200 ng/ml), $1,25(OH)_2D_3$ (VIT D; 10^{-5} unit/ml), dexamethasone (Dexa; 10 ng/ml), or retinoic acid (RA; 2 μM) and harvested at 48 h posttreatment. (F) Relative miR-665 expression was assessed by real-time RT-qPCR in *Runx2*$^{-/-}$ mouse calvarial osteoblast cells. *U6* expression was used as the loading control. EV, empty vector; O-E; overexpressed. (G) *In vivo* occupancy of RUNX2 protein on the miR-337–miR-540–miR665 cluster promoter in mouse osteoblast and rat odontoblast chromatin. Positions of primer and amplified promoter regions are shown in Fig. S2 in the supplemental material. ChIP was performed ($n = 3$) at day 4 of differentiation with anti-RUNX2 and control IgG antibodies; 10% input was used as a positive control. Statistical significance was determined by Student's *t* test (*, $P \leq 0.05$; **, $P \leq 0.01$; ***, $P \leq 0.001$ versus matched control). OB, osteoblast; OdnB, odontoblast.

RUNX2 by overexpression reduced miR-665 overexpression by 50% (Fig. 2F). This result suggests that, in committed odontoblasts, RUNX2 downregulates miR-665 to promote differentiation.

The miR-337–miR-540–miR-665 cluster (miR-337 cluster) is located on human chromosome 14, on mouse chromosome 12, and on rat chromosome 6, upstream of the retrotransposon-like 1 gene (*RTL1*). Human miR-665 has not been fully characterized; however, we found miR-665 expression in human dental pulp cells (Fig. 2B). No information has been published about the promoter region for the miR-337 cluster, and RNA Pol II-mediated transcription of this region has not been characterized. Using bioinformatics, we identified two RUNX2 binding sites in the 5′ upstream region of both the mouse (−300 to −305 and −447 to −452) and the rat (−56 to −61 and −382 to −387) miR-337 cluster, in the proximity of TFIIB and TFIID binding sites (see Fig. S2 in the supplemental material). To assess the *in vivo* binding of RUNX2 to the miR-337 cluster promoter, ChIP assays were performed with mouse osteoblast and rat odontoblast cells. We observed 15% to 20% RUNX2 recruitment in the proximal region (bp −300 to −500 in mouse and bp −200 to −400 in rat) of the miR-337 cluster (Fig. 2G). These results indicate that the downregulation of miR-665 expression results from direct binding by RUNX2. Taken together, these findings indicate that miR-665 has a critical role in the regulation of dentinogenesis that begins in undifferentiated cells, in which low miR-665 expression allows DLX3 to induce odontoblast differentiation (31), and continues with high miR-665 expression attenuating or fine-tuning DLX3 expression during terminal differentiation. Additionally, these results demonstrate a requirement for RUNX2 to negatively regulate miR-665 for progression of osteoblastogenesis.

miR-665 inhibits dentinogenic gene expression. To test our hypothesis that miR-665 regulates DLX3 expression and attenuates odontoblast differentiation, we studied the function of miR-665 *in vitro*. We transduced odontoblast-like OD-21 and MDPC-23 cells with lentivirus vectors encoding GFP and miR-665 or anti-miR-665; infected cells were isolated on the basis of GFP expression (Fig. 3A) and induced to differentiate. In OD-21 odontoblast cells transduced with the miR-665-expressing vector, we observed 7.5- and 7.0-fold upregulation of miR-665 expression at differentiation days 4 and 7, respectively (Fig. 3B). Histochemical staining for ALP, a marker of tooth mineralization, on day 7 revealed that ALP expression was substantially lower in miR-665-overexpressing cells than in control cells (Fig. 3C; see also Fig. S3C

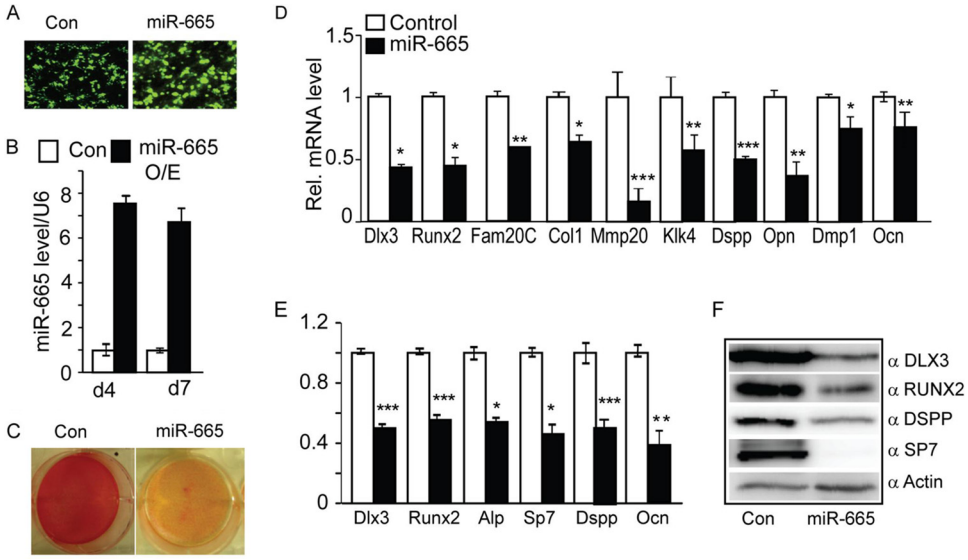

FIG 3 Expression of miR-665 inhibits odontoblast (OD-21) differentiation. (A) Representative fluorescence microscopy images of OD-21 cells infected with control or miR-665-expressing lentivirus vectors for 96 h. GFP is coexpressed with miR-665. (B) Quantitation of the expression levels of miR-665 in OD-21 odontoblast cells infected with miR-665-encoding lentivirus for 24 h, GFP sorted, and cultured in differentiation medium for 4 (d4) or 7 (d7) days. (C) Histochemical staining for ALP activity in OD-21 cells infected with control or miR-665-expressing lentivirus vectors, GFP sorted, and cultured in differentiation medium for 7 days. (D and E) The mRNA expression profile of tooth-related genes in OD-21 GFP-sorted control and miR-665-expressing lentivirus-infected cells detected by PCR after 4 days of differentiation (D) and after 7 days of differentiation (E). (F) Representative Western blot showing the effects of overexpressing miR-665 on the expression levels of DLX3, RUNX2, SP7, and DSPP proteins after 4 days of differentiation with control or miR-665-expressing vectors in GFP-sorted OD-21 cells. Actin was used as the loading control. Con, control; ALP, alkaline phosphatase; Opn, osteopontin; Ocn, osteocalcin; Fam20C, family with sequence similarity 20, member C; Mmp20, matrix metallopeptidase 20; Klk4, kallikrein-related peptidase 4; Dmp1, dentin matrix acidic phosphoprotein 1; Dspp, dentin sialophosphoprotein. Statistical significance was determined by Student's *t* test (*, $P \leq 0.05$; **, $P \leq 0.01$; ***, $P \leq 0.001$ versus matched control). *Gapdh* expression was used as the control.

in the supplemental material), suggesting that miR-665 significantly inhibits odontoblast mineralization.

This result was further supported by analysis of odontoblast-specific markers and regulators of differentiation. On day 4, miR-665 overexpression decreased, whereas anti-miR-665 increased, the expression of *Runx2* and *Dlx3* (Fig. 3D; see also Fig. S3D and E in the supplemental material). Notably, microRNA bioinformatics studies did not reveal miR-665 binding sites in the 3′ UTR of *Runx2* mRNA (http://www.targetscan.org). However, our previous study discovered that DLX3 directly binds to the *Runx2* promoter and activates *Runx2* expression during differentiation (32). Therefore, we conclude that the decrease of *Runx2* expression on day 4 is likely due to the repression of *Dlx3* by miR-665 overexpression rather than to the direct regulation of *Runx2* by miR-665.

Furthermore, miR-665 overexpression significantly decreased, whereas anti-miR-665 increased, the expression of *Col1A1*, *Fam20C*, *Opn*, *Dspp*, *Dmp1*, and *Ocn* on day 4, indicating initial delay of odontoblast maturation and strong inhibition of late mineralization by miR-665 (Fig. 3D; see also Fig. S3E in the supplemental material). We observed similar inhibitory effects of miR-665 overexpression on the expression of *Mmp20* and *Klk4* (Fig. 3D), already reported as downstream targets of *Dlx3* essential for tooth matrix formation (30). Similar inhibition of dentinogenesis was also observed on day 7 of odontoblast differentiation in miR-665-overexpressing cells. Most relevant marker genes were analyzed in evaluating stage-specific tooth development. Expression levels of *Dlx3*, *Runx2*, and *Sp7* transcription factors, required for the maturation odontoblast phenotype, were reduced by 50% (Fig. 3E). Expression levels of *Alp*, an early marker for odontoblast activity, and of *Dspp* and *Ocn*, late markers for odontoblast mineralization, were also significantly decreased (Fig. 3E). These findings indicate that miR-665 strongly inhibits activators essential for progression of odontoblast maturation and mineralization.

We next examined the effects of miR-665 on odontoblast marker proteins. Western blot analysis indicated that RUNX2 protein expression was inhibited severalfold by miR-665 overexpression (Fig. 3F; see also Fig. S3D in the supplemental material). miR-665 overexpression also led to noticeably decreased protein levels of SP7 and DSPP, which are also downstream targets of *Dlx3* and are strong contributors to dentinogenic differentiation (Fig. 3F). These studies provide evidence that *Dlx3* expression is directly controlled through 3′ UTR regulation by miR-665, leading to downregulation of *Runx2*, *Sp7*, *Dspp*, and other target genes to impair dentinogenesis.

miR-665 endogenously associates with members of the chromatin-modifying complex. To study the precise mechanism by which miR-665 contributes to the inhibition of dentinogenesis, we analyzed the components of the RISC. The miR-665-guided RISC was immunoprecipitated from both miR-665-transduced (overexpression) and anti-miR-665-transduced (knockdown) odontoblast-like cells using anti-AGO2 antibody. High-throughput RNA sequencing analysis of immunoprecipitates uncovered 300 significantly altered transcription factors. Among these factors, 60 are chromatin-modifying factors, and of these, 15 are linked to histone acetylation (Fig. 4A; see also Table S5 in the supplemental material), including the *Kat6a* protein. These findings indicate that in odontoblasts miR-665 has a key role in con-

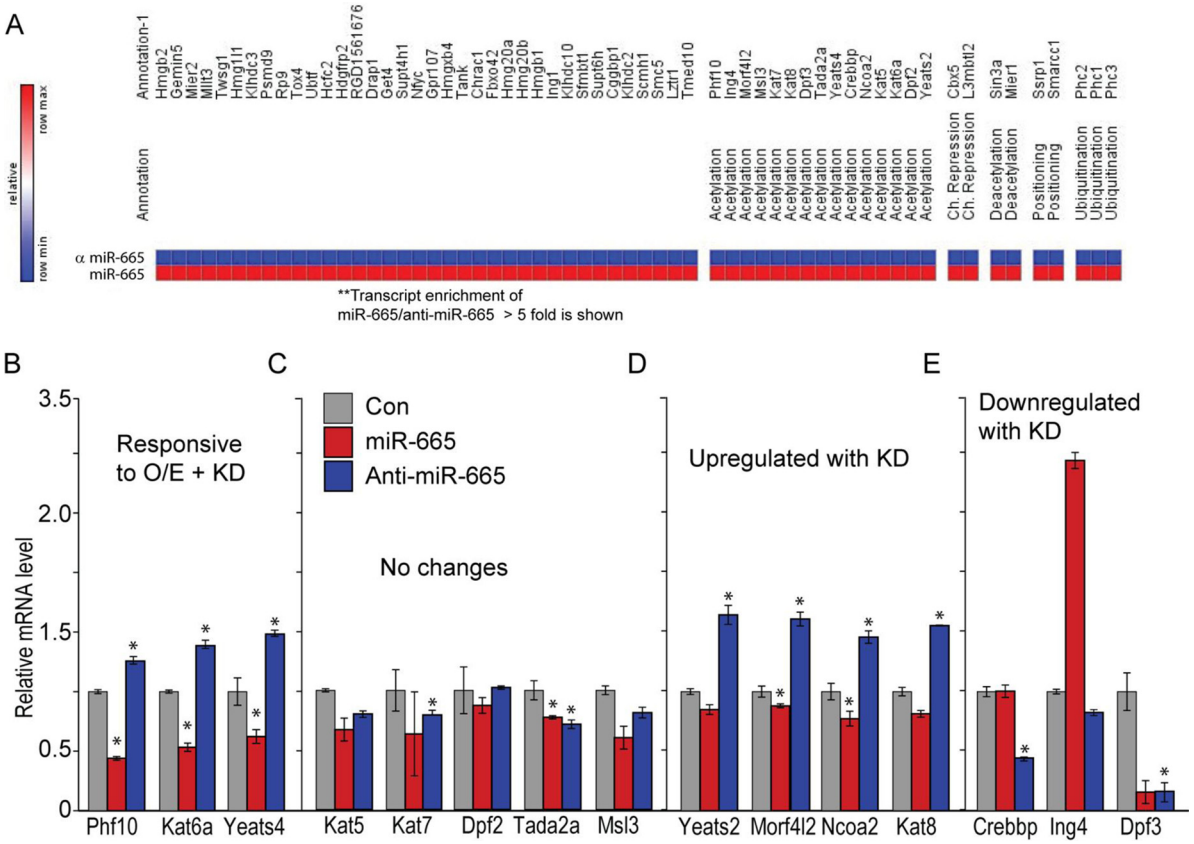

FIG 4 miR-665 associates with chromatin-binding factor *Kat6a* and regulates its expression. (A) AGO2-immunoprecipitated RNA from OD-21 cells overexpressing miR-665, or anti-miR-665 was purified and subjected to RNA sequencing analysis with the Illumina next-generation HiSeq platform. The mRNA transcript abundance in the AGO2 pulldown was normalized to normal IgG. Heat map analysis was performed with GENE-E software (http://www.broadinstitute.org/cancer/software/GENE-E/) and shows the enrichment in cognate mRNA binding to miR-665 over the binding to anti-miR-665. Significant enrichment (>5-fold) of the chromatin-binding factors is shown (red over blue), as noted (**). (B to E) The mRNA expression profile of chromatin-binding factors involved in histone acetylation detected in OD-21 cells infected with control, miR-665-overexpressing, or anti-miR-665-expressing lentivirus vectors and GFP sorted, detected by real-time RT-qPCR after 96 h of infection. O/E, overexpression; KD, knockdown; Con, control; Phf10, PHD finger protein 10; Ing4, inhibitor of growth family, member 4; Morf4l2, mortality factor 4 like 2; Msl3, male-specific lethal 3; Kat, K(lysine) acetyltransferase; Dpf, D4, zinc and double PHD fingers; Tada2a, transcriptional adaptor 2A; Yeats, YEATS domain-containing protein; Crebbp, CREB binding protein; Ncoa2, nuclear receptor coactivator 2; min, minimum; max, maximum. Statistical significance was determined by Student's *t* test (*, $P < 0.01$ versus matched control). *Gapdh* expression was used as the control.

trolling not only *Dlx3* expression but also other potential chromatin-modifying factors that regulate the acetylation of histone H3 and H4 tails of the chromatin of odontoblast-specific genes.

To narrow the list of potential chromatin-modifying factors regulated by miR-665, we confirmed the expression of each by real-time RT-qPCR in miR-665-overexpressing and anti-miR-665-expressing odontoblast-like cells (Fig. 4B to E). We considered only the chromatin factors that were decreased by miR-665 overexpression and increased by miR-665 knockdown. miR-665 overexpression or knockdown significantly altered the expression of PHD finger protein 10 (*Phf10*), *Kat6A*, and YEATS domain-containing protein 4 (*Yeats4*) (Fig. 4B). However, no changes were observed in the expression of *Kat5*, *Kat7*, *Dpf2*, *Tada2a*, or *Msl3* (Fig. 4C). *Dpf3* expression was decreased by either miR-665 overexpression or knockdown (Fig. 4E); however, *Yeats2*, *Morf4l2*, *Ncoa2*, and *Kat8* were upregulated, and *Crebbp* and *Ing4* were downregulated only upon knockdown of miR-665 (Fig. 4D and E). Thus, the expression profiles of *Dpf3*, *Yeats2*, *Ncoa2*, *Morf4l2*, *Kat8*, *Crebbp*, and *Ing4* were not consistent with our criteria for regulation by miR-665 and may be a result of indirect regulation. These results indicate that miR-665 regulates epigenetic factors with histone H3 and H4 acetylation activity to control chromatin remodelling mechanisms and regulate odontoblast differentiation.

To test our hypothesis that the miR-665-regulated changes in the expression of chromatin-binding factors are independent of *Dlx3* downregulation by miR-665, we generated stable DLX3-overexpressing odontoblasts. DLX3 overexpression (see Fig. S4A in the supplemental material) increased the mRNA expression of the DLX3 targets *Runx2* and *Sp7* by 2- and 5-fold, respectively (see Fig. S4B and C); however, no significant increase in the expression of any of the 15 chromatin-binding factors was observed (see Fig. S4D). These results indicate that dentinogenesis is regulated by miR-665-mediated chromatin modification independent of *Dlx3* regulation.

miR-665 directly targets *Kat6a*. Neither the role of *Kat6a* in tooth formation nor the mechanisms by which miR-665 regulates chromatin modifications are understood. To address the mecha-

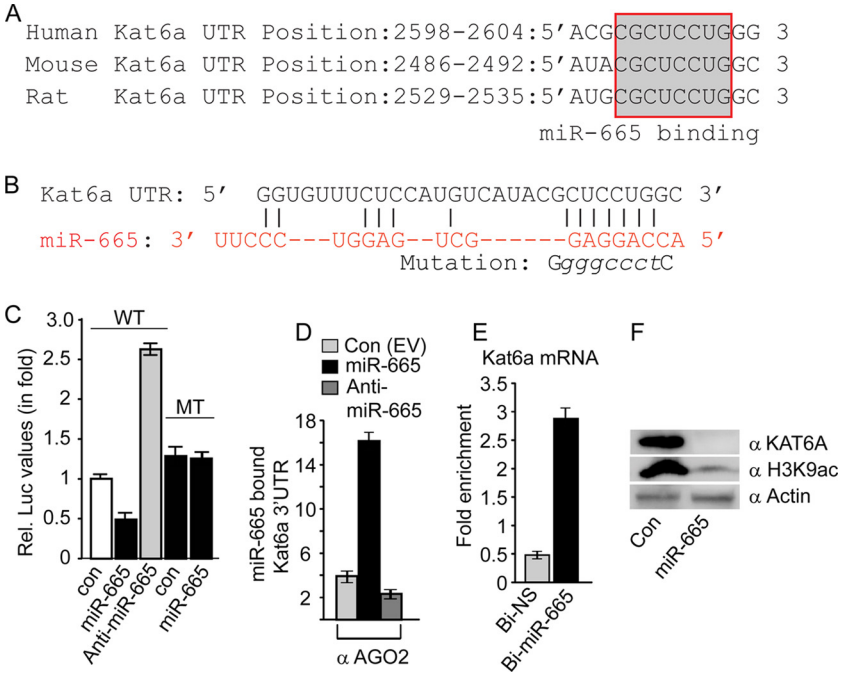

FIG 5 *Kat6a* is a direct target of miR-665. (A) Schematic illustration of the 3′ UTR of *Kat6a* mRNA with a conserved miR-665 binding site. Bioinformatics programs (TargetScan and MicroRNA.org) revealed that the 3′ UTR of murine *Kat6a* has a putative miR-665 binding site. The identified miR-665 binding site (octamer seed sequence, CUCCUGG, is shaded) is evolutionarily conserved among vertebrate species (human, mouse, and rat). (B) *Kat6a* mRNA nucleotide complementarity with the miR-665 seed sequence at the 3′ UTR is illustrated. Lowercase nucleotides indicate the mutations introduced in the seed sequence of the miR-665 binding site. (C) Relative Luc activity in HEK-293T cells transfected with the wild-type (WT) or mutated (MT) *Kat6a* 3′ UTR-Luc reporters along with an NS miRNA control (Con), miR-665, or anti-miR-665. Relative Luc activity was normalized with *Renilla* Luc activity and expressed in relative luminescence units. (D) Quantitative analysis of miR-665 binding to the *Kat6a* mRNA 3′ UTR associated with the RISC was determined by RNA sequencing of AGO2-immunoprecipitated RNA from MDPC-23 dental pulp cells infected with control, miR-665-overexpressing, and anti-miR-665-expressing lentivirus vectors and GFP sorted. Significant changes in transcript expression (*P* values of 0.01 to 0.001) were analyzed using Cuffdiff bioinformatics. (E) Streptavidin pulldown to detect Kat6a mRNA binding to miR-665 in MDPC-23 odontoblast cells transfected with Bi-NS-miR or Bi-miR-665 mimics. The binding of Kat6a mRNA was analyzed by qRT-PCR and normalized to Gapdh expression. (F) Representative Western blot showing KAT6A and acetylated histone H3K9 proteins from MDPC-23 dental pulp cells infected with control or miR-665-overexpressing lentivirus vectors and GFP sorted. Actin was used as the loading control.

nism by which miR-665 regulates epigenetic factor *Kat6a* to control chromatin remodelling mechanisms and regulate odontoblast differentiation, we examined the *Kat6a* 3′ UTR for miR-665 binding sites. Bioinformatics programs revealed a putative miR-665 binding site in the 3′ UTR of murine *Kat6a* that is evolutionarily conserved among vertebrate species (Fig. 5A). *Kat6a* mRNA 3′ UTR and miR-665 nucleotide matching analysis indicated an imperfect mRNA, an miRNA hybrid, appropriate for miR-665-mediated repression (Fig. 5B). We next performed Luc reporter assays to evaluate the binding of miR-665 to the 3′ UTR of *Kat6a* mRNA. miR-665 overexpression substantially reduced the activity (50%) of the *Kat6a* 3′ UTR-Luc reporter in HEK-293T cells (Fig. 5C). However, no change in Luc activity occurred when the miR-665 binding site in the *Kat6a* 3′ UTR was mutated (Fig. 5B, where lowercase nucleotides indicate the mutations introduced in the seed sequence, and C). In contrast, anti-miR-665 overexpression upregulated *Kat6a* 3′ UTR-Luc activity by more than 2-fold. These results indicate that *Kat6a* is directly repressed by miR-665. Furthermore, sequencing of the RNP-IP RNA revealed 8- and 4-fold enrichments in miR-665 binding to the *Kat6a* 3′ UTR in miR-665-overexpressing cells compared with the binding in anti-miR-665- and control lentivirus-overexpressing cells, respectively (Fig. 5D). In Ago2 pulldown RNA, the amplification of miR-665 binding using the UTR-specific primers and miRNA seed sequence-generated cDNA cannot exclude the possibility that the 3′ UTRs of Dlx3 or Kat6a are actually regulated by other miRNAs. Indeed, as a single mRNA can be targeted by multiple miRNAs, it is possible that the Dlx3 or Kat6a binding is mediated by multiple miRNAs, including miR-665. In order to confirm that the 3′ UTRs of Dlx3 and Kat6a mRNA are bound by miR-665, we transfected MDPC-23 cells with biotinylated miR-665 or biotinylated nonspecific miRNA and captured the miR-665-bound mRNAs using streptavidin pulldown of the biotinylated miR-665-mRNA complex. RT-qPCR analysis of streptavidin pulldown RNA indicated 6-fold enrichment of Kat6a mRNA pulled down with Bi-miR-665 over the amount pulled down with the biotinylated nonspecific miRNA (Fig. 5E). To test our hypothesis that miR-665 represses KAT6A translation, thus inhibiting H3K9 acetylation, we examined KAT6A protein expression and H3K9 acetylation levels in miR-665-overexpressing odontoblasts. miR-665 overexpression significantly reduced KAT6A expression and H3K9 acetylation (Fig. 5F). Taken together, these results indicate that miR-665 inhibits odontoblast differentiation by directly targeting *Kat6a* and its histone acetylation activity.

KAT6A interacts with RUNX2, activates tissue-specific promoters, and promotes dentinogenesis. No mechanistic role of *Kat6a* has been defined in tooth formation. However, reports suggest that KAT6A acetylates itself and lysine residues on histones

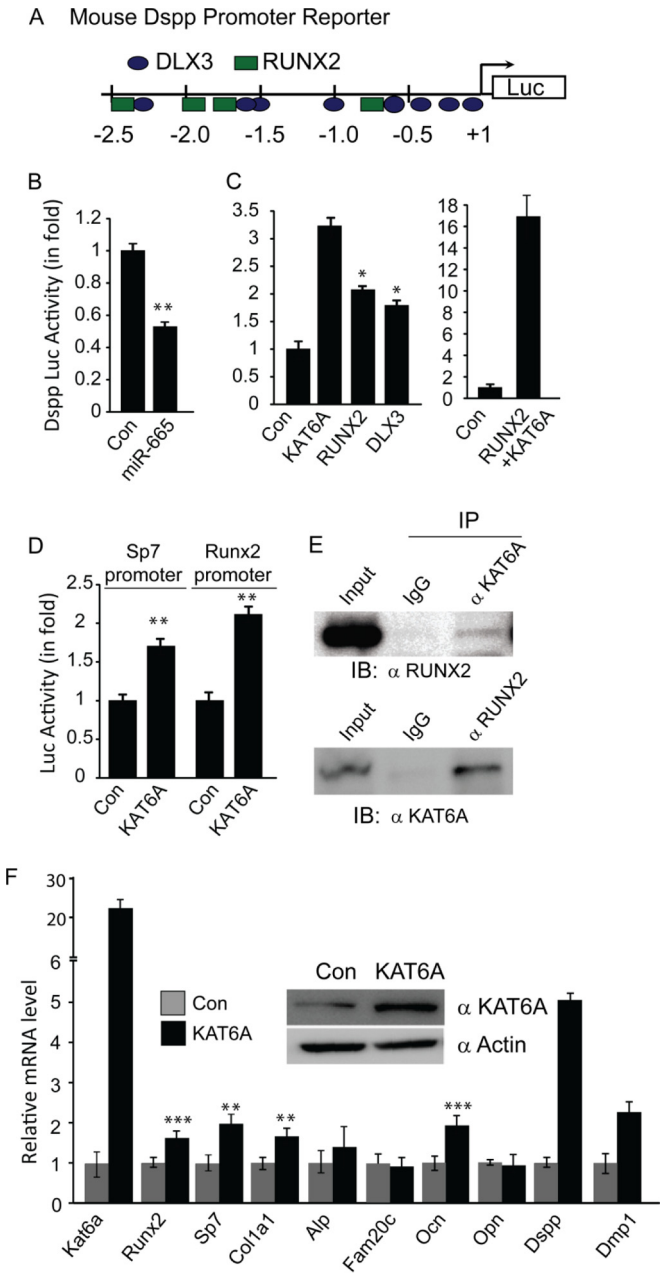

FIG 6 KAT6A promotes odontoblast differentiation. (A) Schematic representation of the 2.5-kb *Dspp* promoter ligated to the pMIR-REPORT Luc reporter gene. The promoter fragment shows putative RUNX2 and DLX3 binding sites containing the core RUNX2 [(T/A)GTGGT or ACCAC(A/T)] and DLX3 (AATTA) motifs. (B) Relative Luc activity in HEK-293T cells transfected with the 2.5-kb *Dspp* promoter-Luc reporter and NS miR control (Con) or miR-665. (C) Relative Luc activity in cells transfected with the 2.5-kb *Dspp* promoter-Luc reporter and *Kat6a*, *Runx2*, or *Dlx3*. (D) Relative Luc activity in cells transfected with the *Sp7* or *Runx2* promoter-Luc reporter and *Kat6a*. Data in panels B and D are presented as mean values ± SEM for three experiments and samples. Experiments were performed in triplicate. Relative Luc activity was normalized with *Renilla* Luc activity and expressed in relative luminescence units. (E) Representative Western blots showing RUNX2 association in KAT6A immunoprecipitates (top) and KAT6A association in RUNX2 immunoprecipitates (bottom). (F) The mRNA expression profile of odontoblast differentiation marker genes in control and KAT6A-overexpressing MDPC-23 cells, detected by real-time RT-PCR after 96 h. A representative Western blot shows exogenous KAT6A expression in MDPC-23 dental pulp cells (inset). Experiments were performed in triplicate, and results are displayed as mean values ± SEM. Con, control; IB, immunoblot; IP, immunoprecipitation; Alp, alkaline phosphatase; Opn, osteopontin; Ocn, osteocalcin; Fam20C, family with sequence similarity 20, member C; Dmp1, dentin matrix acidic phosphoprotein 1; Dspp, dentin sialophosphoprotein; Col1A1, collagen 1α1. Statistical significance was determined by Student's *t* test (*, $P \leq 0.05$; **, $P \leq 0.01$; ***, $P \leq 0.001$ versus matched control). *Gapdh* expression was used as the control.

H2B, H3, and H4 (43–46). Moreover, KAT6A interacts with osteoblast- and odontoblast-specific RUNX2 (43, 51) and has been implicated in skeletogenesis (53). Therefore, we focused on determining how miR-665 regulation is mediated through KAT6A and RUNX2 to control transcriptional and epigenetic changes in bone- and tooth-specific promoters using a *Dspp* promoter reporter assay. Figure 6A illustrates the physical map of the *Dspp* proximal promoter with putative RUNX2 and DLX3 regulatory sites. Promoter activity was reduced by 40% with the overexpression of miR-665 (Fig. 6B). Furthermore, overexpression of RUNX2 or DLX3 increased *Dspp* promoter activity (Fig. 6C). Interestingly, KAT6A overexpression also increased *Dspp* promoter activity, both independently and synergistically with RUNX2 (Fig. 6C, left and right panels), and significantly increased the activity of *Runx2* and *Sp7* promoters (Fig. 6D). Analysis of immunoprecipitates using antibodies against RUNX2 or KAT6A indicated a physical interaction between the two proteins (Fig. 6E). Taken together, these results indicate that KAT6A and RUNX2 functionally cooperate in regulating *Dspp*, and miR-665 hinders this cooperation.

Western blot and real-time RT-qPCR analyses of KAT6A-overexpressing cells confirmed a substantial increase in KAT6A protein expression and a severalfold increase in *Kat6a* mRNA expression (Fig. 6F). Along with the increases in the promoter activity of *Runx2* and *Sp7* reported above (Fig. 6D), KAT6A overexpression increased the mRNA expression of the *Runx2* and *Sp7* transcription factors required for commitment and differentiation, as well as of *Alp*, *Col1a1*, *Ocn*, *Dspp*, and *Dmp1*, the early and late markers of odontoblast matrix maturation and mineralization (Fig. 6F). The substantial upregulation of *Ocn* expression indicates a strong induction of matrix mineralization. Therefore, *Kat6a* appears to be an activator of genes essential for progression of odontoblast maturation and mineralization.

miR-665 inhibits KAT6A binding and histone H3 and H4 acetylation within Dspp and Dmp1 promoters. We next hypothesized that miR-665 alters the *in vivo* binding of KAT6A, RUNX2, and regulators of chromatin remodelling to the *Dspp* and *Dmp1* promoters. We performed ChIP assays in control and miR-665-overexpressing or anti-miR-665-overexpressing cells at differentiation day 7. We observed 10- to 11-fold upregulation in the expression of miR-665 or anti-miR-665 in miR-665 or anti-miR-665 lentivirus-transduced MDPC-23 odontoblast cells (Fig. 7A, left panel). Furthermore, the overexpression of anti-miR-665 decreased the expression levels of endogenous miR-665 by 50% (Fig. 7A, right panel).

We next hypothesized that the translational repression of tooth-specific transcription factors, including DLX3, RUNX2, KAT6A, and SP7, by miR-665 is the decisive factor in whether tooth-specific promoters are activated or repressed. To address this hypothesis, we analyzed protein expression of these factors in miR-665- and anti-miR-665-overexpressing MDPC-23 cells. As shown in Fig. 7B, Western blot analysis revealed that miR-665

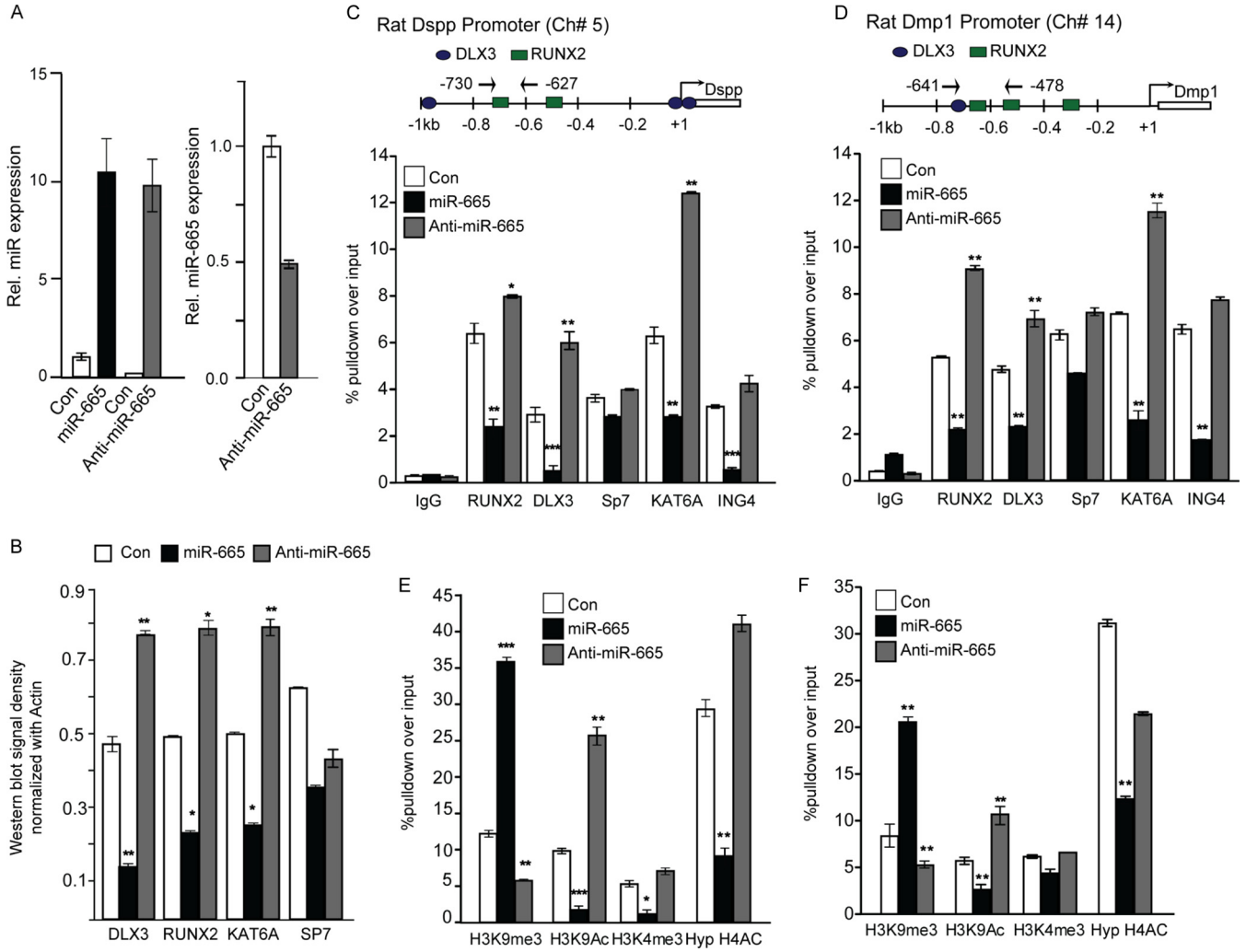

FIG 7 miR-665 decreases the epigenetic marks for transcriptional activation of the *Dspp* and *Dmp1* promoters. (A) Quantitation of the relative expression levels of miR-665 and anti-miR-665 in MDPC-23 odontoblast cells infected with miR-665-overexpressing or anti-miR-665-expressing lentivirus vectors for 96 h (left). The effect of anti-miR-665 expression on miR-665 expression level is also shown (right). (B) Quantitation of DLX3, RUNX2, KAT6A, and SP7 protein expression levels in MDPC-23 cells infected with control, miR-665-overexpressing or anti-miR-665-expressing lentivirus vectors after 96 h of infection ($n = 3$). (C and D) Schematics depicting the primers used in the ChIP assays to amplify the key regulatory elements present in the proximal *Dspp* promoter fragment (C) and the proximal *Dmp1* promoter fragment (D). The arrows indicate the positions of the forward and reverse primers. For the graph, immunoprecipitated DNA samples from ChIP assays with antibodies against indicated transcription factors were amplified by real-time RT-qPCR with gene-specific promoter primers (see Table S3 in the supplemental material). (E and F) Immunoprecipitated DNA samples from ChIP assays with antibodies against indicated histone H3 and H4 modifications were amplified by real-time RT-qPCR with gene-specific promoter primers (see Table S3). ChIP experiments were repeated three times with similar results, and one representative experiment is presented. Statistical significance was determined by Student's *t* test (*, $P \leq 0.05$; **, $P \leq 0.01$; ***, $P \leq 0.001$ versus matched control). IgG was used as a normalization control.

overexpression and knockdown, respectively, decreased and increased DLX3, RUNX2, and KAT6A protein levels. Expression of SP7 protein decreased by 30% to 50% with either miR-665 overexpression or knockdown. We did not identify any miR-665 binding sites in the 3′ UTR of *Sp7* mRNA using miRNA bioinformatics. Therefore, the mechanism controlling downregulation of SP7 protein in the presence of anti-miR-665 is unclear but may involve indirect effects. The proximal promoters of *Dspp* and *Dmp1* were amplified as illustrated in Fig. 7C and D. Recruitment of RUNX2, DLX3, and KAT6A to the *Dspp* and *Dmp1* promoters was significantly lower in miR-665-overexpressing cells, whereas anti-miR-665 expression significantly increased recruitment of these factors (Fig. 7C and D), which indicates that miR-665 mediates transcriptional inhibition of both the *Dspp* and *Dmp1* genes. miR-665 overexpression also scarcely reduced SP7 recruitment to the *Dspp* and *Dmp1* promoters; however, no significant increase in the recruitment of SP7 was found upon miR-665 knockdown. The association of each promoter with ING4, a tumor suppressor with histone H4-specific acetyltransferase activity that is involved in chromatin remodeling (74), was greatly reduced by miR-665 overexpression, but no change was observed with anti-miR-665 expression (Fig. 7C and D). We next examined the histone H3 and H4 modifications in *Dspp* and *Dmp1* chromatin to assess the transcriptional status of these genes. The trimethylation of histone H3 at K9 (H3K9me3) on the *Dspp* and *Dmp1* promoters increased 2- to 3-fold in miR-665-overexpressing cells and decreased 2-fold in

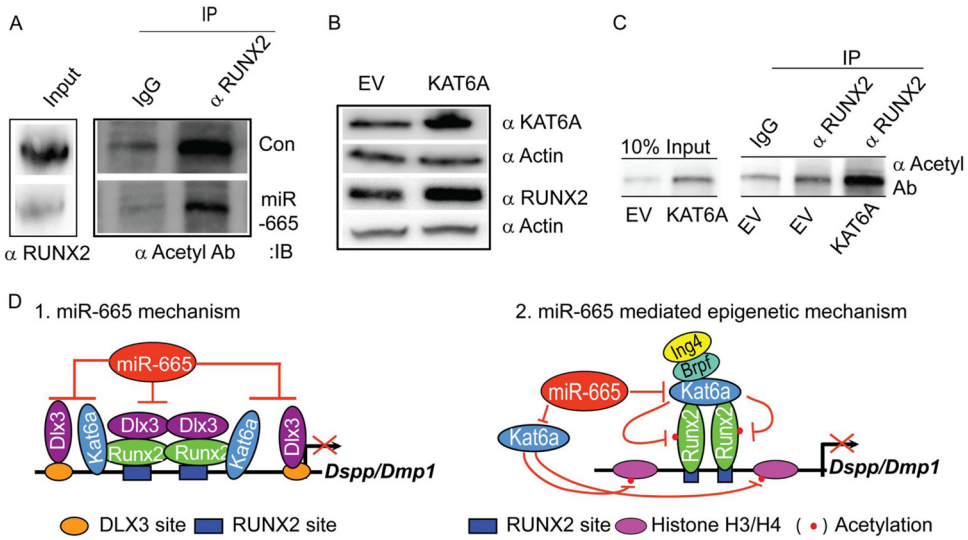

FIG 8 miR-665 inhibits KAT6A-mediated RUNX2 acetylation. (A) Representative Western blot showing RUNX2 immunoprecipitates incubated with anti-acetyl antibody showing the effects of miR-665 overexpression on RUNX2 acetylation in control and miR-665-overexpressing cells. (B) Representative Western blot showing KAT6A and RUNX2 expression in MDPC-23 dental pulp cells transfected with KAT6A. Actin was used as a loading control. (C) Representative Western blot showing RUNX2 immunoprecipitates incubated with anti-acetyl antibody to detect RUNX2 acetylation in KAT6A-overexpressing MDPC-23 dental pulp cells. Normal IgG and empty vector (EV) were used as controls. (D) Two mechanisms of miR-665 regulation of dentinogenesis. Model 1 shows the miRNA-mechanism in which DLX3 and RUNX2 binding and activation of the *Dspp* promoter promote dentinogenesis. miR-665 targets *Dlx3* expression, disrupting the depicted interactions and leading to gene inactivation. Model 2 shows the miRNA-mediated epigenetic mechanism in which KAT6A-mediated acetylation of RUNX2 and chromatin on the *Dspp* promoter activates *Dspp* expression. miRNA-665 represses the expression of *Kat6a*, preventing the acetylation of *Dspp* chromatin and the RUNX2-KAT6A interaction, thus inhibiting *Dspp* expression.

miR-665-knockdown cells, indicating a repressive state of odontoblast differentiation (Fig. 7E and F). In contrast, acetylated histone H3K9 (H3K9ac) and H4 (H4ac) levels were significantly lower in miR-665-overexpressing cells than in control cells. No significant changes in the modifications of acetylated H4 were observed, while acetylated histone H3K9 was strikingly higher in anti-miR-665-overexpressing cells (Fig. 7E and F). Additionally, we observed a 4-fold decrease in the methylation of H3K4me3 on the *Dspp* promoter only (Fig. 7E). These results suggest that miR-665 promotes a repressive state of *Dspp* and *Dmp1* expression as evidenced by higher H3K9me3 recruitment and lower H3K9ac, H4ac, and H3K4me3 recruitment. Thus, miR-665 may actively inhibit H3K9 acetylation by targeting KAT6A and maintaining trimethylation of H3K9. Furthermore, the decreased binding of ING4 and KAT6A likely inhibits formation of activating complexes specific for histone H3 and H4 acetylation on the *Dspp* and *Dmp1* promoters, which would inhibit dentinogenesis.

miR-665 represses KAT6A-mediated RUNX2 acetylation. To test the hypothesis that miR-665 affects the KAT6A acetyltransferase activity involved in the posttranslational acetylation of RUNX2 to inhibit dentinogenesis, we examined anti-RUNX2 immunoprecipitates for acetylation in odontoblast cells overexpressing miR-665 or KAT6A. RUNX2 acetylation was lower in miR-665-overexpressing cells than in control cells (Fig. 8A). These results indicate that the miR-665-induced decrease in DLX3 and KAT6A results in inhibition of RUNX2 protein translation and acetylation. However, from this experimental approach we cannot explain the lower levels of RUNX2 acetylation as miR-665 significantly decreases total RUNX2 protein. To confirm that this effect of miR-665 is mediated through KAT6A, we overexpressed KAT6A in MDPC-23 cells. KAT6A overexpression increased RUNX2 (Fig. 8B) and enriched the acetylation of RUNX2 (Fig. 8C). Thus, miR-665-mediated control of RUNX2 acetylation through KAT6A may be an important component in regulating the differentiation program.

Overall, our results suggest two mechanisms by which miR-665 inhibits odontoblast differentiation (Fig. 8D). (i) In the miR-665 mechanism, miR-665 directly represses expression of the transcription factor DLX3 and its downstream targets (*Runx2*, *Sp7*, *Dspp*, and *Ocn*). The miR-665 target KAT6A also modifies the transcriptional activity of RUNX2 by direct interaction and acetylation. (ii) In the miR-665-mediated epigenetic mechanism, miR-665, through decreased expression of KAT6A, represses tissue-specific *Dspp* and *Dmp1* chromatin by modifying the methylation and acetylation of histone H3 and H4 tails and the alteration of the Moz/Morf histone acetyltransferase complex composition. When taken together, our results provide the first molecular evidence for miR-665 regulation of an miRNA-epigenetic regulatory network to control odontoblast differentiation.

DISCUSSION

Committed preodontoblasts progress through principal stages of differentiation, with each stage characterized by the expression of subsets of miRNAs and genes regulating the smooth transition from the progenitors to mature odontoblasts. Indeed, expression of several miRNAs increases during the late stages of osteoblast differentiation, indicating the importance of miRNA regulation for attenuating continued bone formation at the final osteocyte stage of differentiation (10, 70). However, only a small fraction of the many miRNAs have been evaluated in bone- and tooth-forming cells undergoing differentiation. Here, we identified and functionally characterized a novel *Dlx3*-binding miRNA, miR-665,

that is differentially expressed in odontoblasts and controls the expression of several crucial stage-specific factors to regulate the differentiation program. Specifically, our results indicate that miR-665 functions as a repressor of odontoblast maturation and mineralization by directly repressing the expression of the transcription factor *Dlx3* and, thus, its downstream targets (*Runx2*, *Sp7*, *Dspp*, and *Ocn*). Furthermore, we identified *Kat6a* as an miR-665 target and found that KAT6A also activates and modifies the transcriptional activity of RUNX2 by direct interaction and acetylation. Moreover, miR-665 functions epigenetically through regulation of *Kat6a* to repress tissue-specific *Dspp* and *Dmp1* chromatin remodeling. When taken together, our results provide molecular evidence that miR-665 functions in an miRNA-epigenetic regulatory network to control odontoblast differentiation.

miR-665 and *Dlx3* regulation. *Dlx3* is a member of the distal-less homeobox family that interacts with transcription factors specific to mineralized tissue to regulate craniofacial and postnatal skeletal development (33–43). Our results indicate that there is a cellular requirement for miR-665 to fine-tune the expression of *Dlx3* within physiologic limits for maturation of progenitors to odontoblasts. The very low expression of miR-665 compared with the high expression of DLX3 during proliferation of mouse odontoblasts and human pulp cells and during mouse embryonic bone development indicates that DLX3 promotes dentinogenesis. Therefore, the posttranscriptional regulation of *Dlx3* by miR-665 controlled by BMP2 and RUNX2, as observed in our study, suggests an integrated network of signaling and transcription factors that coordinate the stage-specific events of odontoblast differentiation. This mechanism is consistent with our previous findings that demonstrated selective association of DLX3 and DLX5 with *Runx2* and *Ocn* genes at specific stages of osteoblast maturation as well as participation of these factors and RUNX2 in chromatin remodeling of bone-specific genes (31, 32). Together, these findings emphasize the importance of maintaining appropriate cellular DLX3 levels at each stage of maturation.

miR-665, *Kat6a*, and chromatin regulation. Our results indicate that miR-665 may contribute to alteration of the chromatin status of *Dspp* and *Dmp1* by targeting *Kat6a* expression, which controls the acetylation of histone H3 and H4 tails and alteration of MOZ/MORF complex composition. This suggests that the physiologic modulation of miR-665 levels during differentiation regulates the nucleosome dynamics of dentinogenic-specific markers, including *Dspp* and *Dmp1*, by histone modification. Moreover, our results indicate that KAT6A promotes RUNX2 acetylation and that these proteins function synergistically to increase the transcription of genes involved in dentinogenesis.

The multifunctional role of miR-665 in controlling odontoblast differentiation, including direct targeting of mRNA and the modulation of epigenetic mechanisms through indirect effects on KAT6A recruitment, defines it as a member of a growing master class of specialized miRNAs that control differentiation and tissue development (8, 75, 76). Overall, the linkage of miR-665 to homeodomain factor DLX3, epigenetic factor KAT6A, and transcription factor RUNX2, all three of which regulate tooth biology, supports the developing concept that miRNAs link genetic and epigenetic events that are requisite for maintaining a normal tissue environment. The involvement of miR-665 at multiple levels of odontoblast differentiation suggests diverse functions for miR-665 that include physiologic tooth formation and homeostasis and may inform the design of therapeutics for dental disorders.

ACKNOWLEDGMENTS

We thank the members of the Institute of Oral Health Research for assistance with experimentation, critical comments, technical advice, and sharing of reagents and/or general support as well as Erin E. Thacker for editing the manuscript. We gratefully acknowledge the receipt of OD-21 and MDPC-23 cells from Tatiana Botero and Jacques E. Nör (University of Michigan School of Density, MI). We also thank Michael R. Crowley and David K. Crossman of UAB Heflin Centre for Genomic Sciences for RNA sequencing analyses.

We declare that we have no conflicts of interest.

REFERENCES

1. **Huang XF, Chai Y.** 2012. Molecular regulatory mechanism of tooth root development. Int J Oral Sci **4:**177–181. http://dx.doi.org/10.1038/ijos.2012.61.
2. **Liu H, Lin Huang XF, Chai H, Zhang L, Sun Q, Yuan G, Zhang L, Chen S, Chen Z.** 2013. MiR-145 and miR-143 regulate odontoblast differentiation through targeting Klf4 and Osx genes in a feedback loop. J Biol Chem **288:**9261-9271. http://dx.doi.org/10.1074/jbc.M112.433730.
3. **Lee RC, Feinbaum RL, Ambros V.** 1993. The C. elegans heterochronic gene *lin-4* encodes small RNAs with antisense complementarity to *lin-14*. Cell **75:**843-854. http://dx.doi.org/10.1016/0092-8674(93)90529-Y.
4. **Wightman B, Ha I, Ruvkun G.** 1993. Posttranscriptional regulation of the heterochronic gene *lin-14* by *lin-4* mediates temporal pattern formation in *C. elegans*. Cell **75:**855-862. http://dx.doi.org/10.1016/0092-8674(93)90530-4.
5. **Bartel DP.** 2004. MicroRNAs: genomics, biogenesis, mechanism, and function. Cell **116:**281-297. http://dx.doi.org/10.1016/S0092-8674(04)00045-5.
6. **Leonardo TR, Schultheisz HL, Loring JF, Laurent LC.** 2012. The functions of microRNAs in pluripotency and reprogramming. Nat Cell Biol **14:**1114-1121. http://dx.doi.org/10.1038/ncb2613.
7. **Hermeking H.** 2012. MicroRNAs in the p53 network: micromanagement of tumor suppression. Nat Rev Cancer **12:**613-626. http://dx.doi.org/10.1038/nrc3318.
8. **Liu N, Olson EN.** 2010. MicroRNA regulatory networks in cardiovascular development. Dev Cell **18:**510-525. http://dx.doi.org/10.1016/j.devcel.2010.03.010.
9. **Ebert MS, Sharp PA.** 2012. Roles for microRNAs in conferring robustness to biological processes. Cell **149:**515-524. http://dx.doi.org/10.1016/j.cell.2012.04.005.
10. **Lian JB, Stein GS, van Wijnen AJ, Stein JL, Hassan MQ, Gaur T, Zhang Y.** 2012. MicroRNA control of bone formation and homeostasis. Nat Rev Endocrinol **8:**212-227. http://dx.doi.org/10.1038/nrendo.2011.234.
11. **Kobayashi T, Lu J, Cobb BS, Rodda SJ, McMahon AP, Schipani E, Merkenschlager M, Kronenberg HM.** 2008. Dicer-dependent pathways regulate chondrocyte proliferation and differentiation. Proc Natl Acad Sci U S A **105:**1949-1954. http://dx.doi.org/10.1073/pnas.0707900105.
12. **Murchison EP, Partridge JF, Tam OH, Cheloufi S, Hannon GJ.** 2005. Characterization of Dicer-deficient murine embryonic stem cells. Proc Natl Acad Sci U S A **102:**12135-12140. http://dx.doi.org/10.1073/pnas.0505479102.
13. **Gaur T, Hussain S, Mudhasani R, Parulkar I, Colby JL, Frederick D, Kream BE, van Wijnen AJ, Stein JL, Stein GS, Jones SN, Lian JB.** 2010. Dicer inactivation in osteoprogenitor cells compromises fetal survival and bone formation, while excision in differentiated osteoblasts increases bone mass in the adult mouse. Dev Biol **340:**10-21. http://dx.doi.org/10.1016/j.ydbio.2010.01.008.
14. **Wu Q, Song R, Ortogero N, Zheng H, Evanoff R, Small CL, Griswold MD, Namekawa SH, Royo H, Turner JM, Yan W.** 2012. The RNase III enzyme DROSHA is essential for microRNA production and spermatogenesis. J Biol Chem **287:**25173-25190. http://dx.doi.org/10.1074/jbc.M112.362053.
15. **O'Carroll D, Mecklenbrauker I, Das PP, Santana A, Koenig U, Enright AJ, Miska EA, Tarakhovsky A.** 2007. A Slicer-independent role for Argonaute 2 in hematopoiesis and the microRNA pathway. Genes Dev **21:**1999-2004. http://dx.doi.org/10.1101/gad.1565607.
16. **Mizoguchi F, Izu Y, Hayata T, Hemmi H, Nakashima K, Nakamura T, Kato S, Miyasaka N, Ezura Y, Noda M.** 2010. Osteoclast-specific Dicer gene deficiency suppresses osteoclastic bone resorption. J Cell Biochem **109:**866-875. http://dx.doi.org/10.1002/jcb.22228.
17. **Cao H, Wang J, Li X, Florez S, Huang Z, Venugopalan SR, Elangovan**

S, Skobe Z, Margolis HC, Martin JF, Amendt BA. 2010. MicroRNAs play a critical role in tooth development. J Dent Res **89:**779-784. http://dx.doi.org/10.1177/0022034510369304.
18. **Cao H, Jheon A, Li X, Sun Z, Wang J, Florez S, Zhang Z, McManus MT, Klein OD, Amendt BA.** 2013. The Pitx2: miR-200c/141:noggin pathway regulates Bmp signaling and ameloblast differentiation. Development **140:**3348–3359. http://dx.doi.org/10.1242/dev.089193.
19. **Sharp T, Wang J, Li X, Cao H, Gao S, Moreno M, Amendt BA.** 2014. A pituitary homeobox 2 (Pitx2): microRNA-200a-3p: beta-catenin pathway converts mesenchyme cells to amelogenin-expressing dental epithelial cells. J Biol Chem **289:**27327–27341. http://dx.doi.org/10.1074/jbc.M114.575654.
20. **Li A, Song T, Wang F, Liu D, Fan Z, Zhang C, He J, Wang S.** 2012. MicroRNAome and expression profile of developing tooth germ in miniature pigs. PLoS One **7:**e52256. http://dx.doi.org/10.1371/journal.pone.0052256.
21. **Khan QE, Sehic A, Khuu C, Risnes S, Osmundsen H.** 2013. Expression of Clu and Tgfb1 during murine tooth development: effects of in-vivo transfection with anti-miR-214. Eur J Oral Sci **121:**303–312. http://dx.doi.org/10.1111/eos.12056.
22. **Sun F, Wan M, Xu X, Gao B, Zhou Y, Sun J, Cheng L, Klein OD, Zhou X, Zheng L.** 2014. Crosstalk between miR-34a and notch signalling promotes differentiation in apical papilla stem cells (SCAPs). J Dent Res **93:**589–595. http://dx.doi.org/10.1177/0022034514531146.
23. **Wan M, Gao B, Sun F, Tang Y, Ye L, Fan Y, Klein OD, Zhou X, Zheng L.** 2012. MicroRNA miR-34a regulates cytodifferentiation and targets multi-signalling pathways in human dental papilla cells. PLoS One **7:**e50090. http://dx.doi.org/10.1371/journal.pone.0050090.
24. **Kim EJ, Lee MJ, Li L, Yoon KS, Kim KS, Jung HS.** 2014. Failure of tooth formation mediated by miR-135a overexpression via BMP signaling. J Dent Res **93:**571–575. http://dx.doi.org/10.1177/0022034514529303.
25. **Park MG, Kim JS, Park SY, Lee SA, Kim HJ, Kim CS, Kim JS, Chun HS, Park JC, Kim do, K.** 2014. MicroRNA-27 promotes the differentiation of odontoblastic cell by targeting APC and activating Wnt/β-catenin signaling. Gene **538:**266–272. http://dx.doi.org/10.1016/j.gene.2014.01.045.
26. **Chen P, Wei D, Xie B, Ni J, Xuan D, Zhang J.** 2014. Effect and possible mechanism of network between microRNAs and RUNX2 gene on human dental follicle cells. J Cell Biochem **115:**340–348. http://dx.doi.org/10.1002/jcb.24668.
27. **Zhong N, Sun J, Min Z, Zhao W, Zhang R, Wang W, Tian J, Tian L, Ma J, Li D, Han Y, Lu S.** 2012. MicroRNA-337 is associated with chondrogenesis through regulating TGFBR2 expression. Osteoarthritis Cartilage **20:**593–602. http://dx.doi.org/10.1016/j.joca.2012.03.002.
28. **Morasso MI, Grinberg A, Robinson G, Sargent TD, Mahon KA.** 1999. Placental failure in mice lacking the homeobox gene Dlx3. Proc Natl Acad Sci U S A **96:**162–167. http://dx.doi.org/10.1073/pnas.96.1.162.
29. **Duverger O, Isaac J, Zah A, Hwang J, Berdal A, Lian JB, Morasso MI.** 2013. *In vivo* impact of Dlx3 conditional inactivation in neural crest-derived craniofacial bones. J Cell Physiol **228:**654–664. http://dx.doi.org/10.1002/jcp.24175.
30. **Duverger O, Zah A, Isaac J, Sun HW, Bartels AK, Lian JB, Berdal A, Hwang J, Morasso MI.** 2012. Neural crest deletion of Dlx3 leads to major dentin defects through down-regulation of Dspp. J Biol Chem **287:**12230–12240. http://dx.doi.org/10.1074/jbc.M111.326900.
31. **Hassan MQ, Javed A, Morasso MI, Karlin J, Montecino M, van Wijnen AJ, Stein GS, Stein JL, Lian JB.** 2004. Dlx3 transcriptional regulation of osteoblast differentiation: temporal recruitment of Msx2, Dlx3, and Dlx5 homeodomain proteins to chromatin of the osteocalcin gene. Mol Cell Biol **24:**9248–9261. http://dx.doi.org/10.1128/MCB.24.20.9248-9261.2004.
32. **Hassan MQ, Tare RS, Lee SH, Mandeville M, Morasso MI, Javed A, van Wijnen AJ, Stein JL, Stein GS, Lian JB.** 2006. BMP2 commitment to the osteogenic lineage involves activation of Runx2 by DLX3 and a homeodomain transcriptional network. J Biol Chem **281:**40515–40526. http://dx.doi.org/10.1074/jbc.M604508200.
33. **Li X, Yang G, Fan M.** 2012. Effects of homeobox gene distal-less 3 on proliferation and odontoblastic differentiation of human dental pulp cells. J Endod **38:**1504–1510. http://dx.doi.org/10.1016/j.joen.2012.07.009.
34. **Viale-Bouroncle S, Felthaus O, Schmalz G, Brockhoff G, Reichert TE, Morsczeck C.** 2012. The transcription factor DLX3 regulates the osteogenic differentiation of human dental follicle precursor cells. Stem Cells Dev **21:**1936–1947. http://dx.doi.org/10.1089/scd.2011.0422.
35. **Choi SJ, Roodman GD, Feng JQ, Song IS, Amin K, Hart PS, Wright JT, Haruyama N, Hart TC.** 2009. *In vivo* impact of a 4-bp deletion mutation in the DLX3 gene on bone development. Dev Biol **325:**129–137. http://dx.doi.org/10.1016/j.ydbio.2008.10.014.
36. **Choi SJ, Song IS, Feng JQ, Gao T, Haruyama N, Gautam P, Robey PG, Hart TC.** 2010. Mutant DLX 3 disrupts odontoblast polarization and dentin formation. Dev Biol **344:**682–692. http://dx.doi.org/10.1016/j.ydbio.2010.05.499.
37. **Duverger O, Lee D, Hassan MQ, Chen SX, Jaisser F, Lian JB, Morasso MI.** 2008. Molecular consequences of a frame shifted DLX3 mutant leading to tricho-dento-osseous syndrome. J Biol Chem **283:**20198–20208. http://dx.doi.org/10.1074/jbc.M709562200.
38. **Dong J, Amor D, Aldred MJ, Gu T, Escamilla M, MacDougall M.** 2005. DLX3 mutation associated with autosomal dominant amelogenesis imperfecta with taurodontism. Am J Med Genet A. **133A:**138–141. http://dx.doi.org/10.1002/ajmg.a.30521.
39. **Haldeman RJ, Cooper LF, Hart TC, Phillips C, Boyd C, Lester GE, Wright JT.** 2004. Increased bone density associated with DLX3 mutation in the tricho-dento-osseous syndrome. Bone **35:**988–997. http://dx.doi.org/10.1016/j.bone.2004.06.003.
40. **Beanan MJ, Sargent TD.** 2000. Regulation and function of Dlx3 in vertebrate development. Dev Dyn **218:**545–553. http://dx.doi.org/10.1002/1097-0177(2000)9999:9999<::AID-DVDY1026>3.0.CO;2-B.
41. **Isaac J, Erthal J, Gordon J, Duverger O, Sun HW, Lichtler AC, Stein GS, Lian JB, Morasso MI.** 2014. DLX3 regulates bone mass by targeting genes supporting osteoblast differentiation and mineral homeostasis in vivo. Cell Death Differ **21:**1365–1376. http://dx.doi.org/10.1038/cdd.2014.82.
42. **Marchler-Bauer A, Zheng C, Chitsaz F, Derbyshire MK, Geer LY, Geer RC, Gonzales NR, Gwadz M, Hurwitz DI, Lanczycki CJ, Lu F, Lu S, Marchler GH, Song JS, Thanki N, Yamashita RA, Zhang D, Bryant SH.** 2013. CDD: conserved domains and protein three-dimensional structure. Nucleic Acids Res **41:**D348–D52. http://dx.doi.org/10.1093/nar/gks1243.
43. **Champagne N, Pelletier N, Yang XJ.** 2001. The monocytic leukemia zinc finger protein MOZ is a histone acetyltransferase. Oncogene **20:**404–409.
44. **Kitabayashi I, Aikawa Y, Nguyen LA, Yokoyama A, Ohki M.** 2001. Activation of AML1-mediated transcription by MOZ and inhibition by the MOZ-CBP fusion protein. EMBO J **20:**7184–7196. http://dx.doi.org/10.1093/emboj/20.24.7184.
45. **Holbert MA, Sikorski T, Carten J, Snowflack D, Hodawadekar S, Marmorstein R.** 2007. The human monocytic leukemia zinc finger histone acetyltransferase domain contains DNA-binding activity implicated in chromatin targeting. J Biol Chem **282:**36603–36613. http://dx.doi.org/10.1074/jbc.M705812200.
46. **Thomas T, Corcoran LM, Gugasyan R, Dixon MP, Brodnicki T, Nutt SL, Metcalf D, Voss AK.** 2006. Monocytic leukemia zinc finger protein is essential for the development of long-term reconstituting hematopoietic stem cells. Genes Dev **20:**1175–1186. http://dx.doi.org/10.1101/gad.1382606.
47. **Yoshida H, Kitabayashi I.** 2008. Chromatin regulation by AML1 complex. Int J Hematol **87:**19–24. http://dx.doi.org/10.1007/s12185-007-0004-0.
48. **Paggetti J, Largeot A, Aucagne R, Jacquel A, Lagrange B, Yang XJ, Solary E, Bastie JN, Delva L.** 2010. Crosstalk between leukemia-associated proteins MOZ and MLL regulates HOX gene expression in human cord blood $CD34^+$ cells. Oncogene **29:**5019–5031. http://dx.doi.org/10.1038/onc.2010.254.
49. **Katsumoto T, Aikawa Y, Iwama A, Ueda S, Ichikawa H, Ochiya T, Kitabayashi I.** 2006. MOZ is essential for maintenance of hematopoietic stem cells. Genes Dev **20:**1321–1330. http://dx.doi.org/10.1101/gad.1393106.
50. **Soung do, Y, Talebian L, Matheny CJ, Guzzo R, Speck ME, Lieberman JR, Speck NA, Drissi H.** 2012. Runx1 dose-dependently regulates endochondral ossification during skeletal development and fracture healing. J Bone Miner Res **27:**1585–1597. http://dx.doi.org/10.1002/jbmr.1601.
51. **Pelletier N, Champagne N, Stifani S, Yang XJ.** 2002. MOZ and MORF histone acetyltransferases interact with the Runt-domain transcription factor Runx2. Oncogene **21:**2729–2740. http://dx.doi.org/10.1038/sj.onc.1205367.
52. **Komori T, Yagi H, Nomura S, Yamaguchi A, Sasaki K, Deguchi K, Shimizu Y, Bronson RT, Gao YH, Inada M, Sato M, Okamoto R, Kitamura Y, Yoshiki S, Kishimoto T.** 1997. Targeted disruption of Cbfa1 results in a complete lack of bone formation owing to maturational arrest of osteoblasts. Cell **89:**755–764. http://dx.doi.org/10.1016/S0092-8674(00)80258-5.
53. **Komori T.** 2008. Regulation of bone development and maintenance by Runx2. Front Biosci **13:**898–903. http://dx.doi.org/10.2741/2730.
54. **Voss AK, Collin C, Dixon MP, Thomas T.** 2009. Moz and retinoic acid

coordinately regulate H3K9 acetylation, *hox* gene expression, and segment identity. Dev Cell **17:**674–686. http://dx.doi.org/10.1016/j.devcel.2009.10.006.

55. **Voss AK, Vanyai HK, Collin C, Dixon MP, McLennan TJ, Sheikh BN, Scambler P, Thomas T.** 2012. MOZ regulates the Tbx1 locus, and Moz mutation partially phenocopies Di-George syndrome. Dev Cell **23:**652–663. http://dx.doi.org/10.1016/j.devcel.2012.07.010.
56. **Perez-Campo FM, Costa G, Lie-a Ling M, Kouskoff V, Lacaud G.** 2013. The MYSTerious MOZ, a histone acetyltransferase with a key role in haematopoiesis. Immunology **139:**161–165. http://dx.doi.org/10.1111/imm.12072.
57. **Botero TM, Mantellini MG, Song W, Hanks CT, Nör JE.** 2003. Effect of lipopolysaccharides on vascular endothelial growth factor expression in mouse pulp cells and macrophages. Eur J Oral Sci **111:**228–234. http://dx.doi.org/10.1034/j.1600-0722.2003.00041.x.
58. **Unterbrink A, O'Sullivan M, Chen S, MacDougall M.** 2002. TGFβ-1 downregulates DMP-1 and DSPP in odontoblasts. Connect Tissue Res **43:**354–358. http://dx.doi.org/10.1080/03008200290000565.
59. **Hassan MQ, Gordon JA, Lian JB, van Wijnen AJ, Stein JL, Stein GS.** 2010. Ribonucleoprotein immunoprecipitation (RNP-IP): a direct in vivo analysis of microRNA-targets. J Cell Biochem **110:**817–822. http://dx.doi.org/10.1002/jcb.22562.
60. **Hafner M, Lianoglou S, Tuschl T, Betel D.** 2012 Genome-wide identification of miRNA targets by PAR-CLIP. Methods **58:**94–105. http://dx.doi.org/10.1016/j.ymeth.2012.08.006.
61. **Hafner M, Ascano M, Jr, Tuschl T.** 2011. New insights in the mechanism of microRNA-mediated target repression. Nat Struct Mol Biol **18:**1181–1182. http://dx.doi.org/10.1038/nsmb.2170.
62. **Friedländer MR, Mackowiak SD, Li N, Chen W, Rajewsky N.** 2012. miRDeep2 accurately identifies known and hundreds of novel microRNA genes in seven animal clades. Nucleic Acids Res **40:**37–52. http://dx.doi.org/10.1093/nar/gkr688.
63. **Ender C, Krek A, Friedländer MR, Beitzinger M, Weinmann L, Chen W, Pfeffer S, Rajewsky N, Meister G.** 2008. A human snoRNA with microRNA-like functions. Mol Cell **32:**519–528. http://dx.doi.org/10.1016/j.molcel.2008.10.017.
64. **Chi SW, Zang JB, Mele A, Darnell RB.** 2009. Argonaute HITS-CLIP decodes microRNA-mRNA interaction maps. Nature **460:**479–486. http://dx.doi.org/10.1038/nature08170.
65. **Leung AK, Young AG, Bhutkar A, Zheng GX, Bosson AD, Nielsen CB, Sharp PA.** 2011. Genome-wide identification of Ago2 binding sites from mouse embryonic stem cells with and without mature microRNAs. Nat Struct Mol Biol **18:**237–244. http://dx.doi.org/10.1038/nsmb.1991.
66. **Riley KJ, Yario TA, Steitz JA.** 2012. Association of Argonaute proteins and microRNAs can occur after cell lysis. RNA **18:**1581–1585. http://dx.doi.org/10.1261/rna.034934.112.
67. **Cho J, Chang H, Kwon SC, Kim B, Kim Y, Choe J, Ha M, Kim YK, Kim VN.** 2012. LIN28A is a suppressor of ER-associated translation in embryonic stem cells. Cell **151:**765–777. http://dx.doi.org/10.1016/j.cell.2012.10.019.
68. **Ørom UA, Lund AH.** 2007. Isolation of microRNA targets using biotinylated synthetic microRNAs. Methods **43:**162–165. http://dx.doi.org/10.1016/j.ymeth.2007.04.007.
69. **Ørom UA, Nielsen Lund FC, AH.** 2008. MicroRNA-10a binds the 5′ UTR of ribosomal protein mRNAs and enhances their translation. Mol Cell **30:**460–471. http://dx.doi.org/10.1016/j.molcel.2008.05.001.
70. **Hassan MQ, Gordon JA, Beloti MM, Croce CM, van Wijnen AJ, Stein JL, Stein GS, Lian JB.** 2010. A network connecting Runx2, SATB2, and the miR-23a∼27a∼24-2 cluster regulates the osteoblast differentiation program. Proc Natl Acad Sci U S A **107:**19879–19884. http://dx.doi.org/10.1073/pnas.1007698107.
71. **John B, Enright AJ, Aravin A, Tuschl T, Sander C, Marks DS.** 2004. Human microRNA targets. PLoS Biol **2:**e363. http://dx.doi.org/10.1371/journal.pbio.0020363.
72. **Xu J, Li CX, Li YS, Lv JY, Ma Y, Shao TT, Xu LD, Wang YY, Du L, Zhang YP, Jiang W, Li CQ, Xiao Y, Li X.** 2011. MiRNA-miRNA synergistic network: construction via co-regulating functional modules and disease miRNA topological features. Nucleic Acids Res **39:**825–836. http://dx.doi.org/10.1093/nar/gkq832.
73. **Bartel DP.** 2009. MicroRNAs: target recognition and regulatory functions. Cell **136:**215–233. http://dx.doi.org/10.1016/j.cell.2009.01.002.
74. **Doyon Y, Cayrou C, Ullah M, Landry AJ, Cote V, Selleck W, Lane WS, Tan S, Yang XJ, Cote J.** 2006. ING tumor suppressor proteins are critical regulators of chromatin acetylation required for genome expression and perpetuation. Mol Cell **21:**51–64. http://dx.doi.org/10.1016/j.molcel.2005.12.007.
75. **Botchkareva NV.** 2012. MicroRNA/mRNA regulatory networks in the control of skin development and regeneration. Cell Cycle **11:**468–474. http://dx.doi.org/10.4161/cc.11.3.19058.
76. **Bengestrate L, Virtue S, Campbell M, Vidal-Puig A, Hadaschik D, Hahn P, Bielke W.** 2011. Genome-wide profiling of microRNAs in adipose mesenchymal stem cell differentiation and mouse models of obesity. PLoS One **6:**e21305. http://dx.doi.org/10.1371/journal.pone.0021305.